Double Distribution of Dark Matter Halos with respect to Mass and Local Overdensity

Vasiliki Pavlidou and Brian D. Fields
Center for Theoretical Astrophysics, Department of Astronomy
University of Illinois, Urbana, IL 61801
(Dated: October 14, 2004)

We present a double distribution function of dark matter halos, with respect to both object mass and local over- (or under-) density. This analytical tool provides a statistical treatment of the properties of matter *surrounding* collapsed objects, and can be used to study environmental effects on hierarchical structure formation. The size of the "local environment" of a collapsed object is defined to depend on the mass of the object. The Press-Schechter mass function is recovered by integration of our double distribution over the density contrast. We also present a detailed treatment of the evolution of overdensities *and underdensities* in $\Omega_{\rm m}+\Omega_\Lambda=1$ and $\Omega_{\rm m}=1$ universes according to the spherical evolution model. We explicitly distinguish between true and linearly extrapolated overdensities and provide conversion relations between the two quantities.

PACS numbers: 98.80.-k; 95.35.+d; 98.65.-r

I. INTRODUCTION

Cosmological distributions have long been used with great success as an analytical tool complementary to numerical simulations. They have been used to constrain the cosmological parameters; interpret results of cosmological simulations; study regions of the parameter space which cannot be approached by simulations due to prohibitive computational cost; exploring the effects of various physical processes in an efficient if approximate way. The analytical tool used most widely in cosmology is the mass function of dark matter halos (distribution of the number density of halos with respect to halo mass). Analytical descriptions of dark matter halos are usually based on the Press-Schechter formalism ([1],[2]) and its extensions (e.g.,[3], [4], [5], [6]). The Press-Schechter mass function has is in good agreement with the results of N-body simulations (e.g. [7], [8], [9]). More sophisticated approaches taking into account deviations from spherical symmetry (e.g., [10], [11],[12]) have improved this agreement even further.

To derive the Press-Schechter mass function, regions in space are smoothed on successively smaller scales. The mass of a collapsed object is then taken to be the largest smoothing mass scale for which the average linear overdensity exceeds some threshold. In this way, matter in the universe is distributed among collapsed structures of different masses, which all share the same value of average overdensity (the threshold value). Information about the local environment of the collapsed objects (whether they live in underdensities or overdensities) is thus erased.

For this reason, and despite its wide applicability, the expression for the mass function cannot be used to address environment-related questions: Does the mass function of structures in superclusters differ from the mass function inside voids? Are structures of some particular mass more likely to reside inside underdense or overdense regions in space? How does such a preference evolve with redshift, and how sensitively does it depend on the cosmological parameters? How does the state of the material surrounding and accreted by a collapsed object depend on the mass of the object and the cosmic epoch?

To address such questions, we seek a *double distribution* of the number density of structures with respect to mass but also to local overdensity (or underdensity). In order to extract information about the surroundings of collapsed structures, we use the same random walk formalism which rigorously yields the Press-Schechter mass function ([2], [3]). Integration of this distribution over density contrast should return the Press-Schechter mass function so that the successes of the Press-Schechter formalism be retained.

Two complications arise in the effort to expand the Press-Schechter mass function to incorporate a description of the local overdensity. First, the concept of the "local environment" is somewhat vague and needs to be defined in a more rigorous way. The size of the "local environment" cannot be the same for all structures. If this was the case, very small structures would represent only a tiny fraction of the "environment", while very large structures could even exceed the size of the "environment", which would be an unphysical situation. This problem is not exclusive to analytical tools, but also needs to be addressed when analyzing the results of numerical simulations. Second, the Press-Schechter treatment of the density field uses linear theory, and ways of converting this information to a more physical non-linear result need to be determined.

We address the first problem by introducing a *clustering scale parameter*, β, which allows us to define the size of the "environment" of each structure as a function of its mass. We address the second concern by calculating conversion relations between the linear-theory overdensities (or underdensities) and those predicted by the spherical-evolution model.

Environment-related questions in cosmological structure formation have also beed addressed using analytical

models for the clustering properties of dark halos which evaluate quantities such as the cross-correlation function between dark halos and matter, and the biasing factor (e.g. [13], [14], [15], [16], [17], [18], [19], also see review by [20] and references therein). These analyses are based on the same random walk formalism which we use here to derive our double distribution (also see [21] for fitting formulae from N-body simulation results). However, the information content of the double distribution, which treats the "environment" in a mass-dependent fashion, is complementary to that of correlation functions, which describe the clustering properties of the dark halo population at some *fixed spatial scale*. The double distribution is ideally fitted for population studies of cosmological objects. If the properties of a single object can be parametrized as a function of its mass and its environment, then the double distribution can be used to predict the statistical properties of such objects, as well as their evolution with time, for any cosmological model.

Our paper is organized as follows. In §II we briefly review the "random walk" formalism used in the derivation of the Press-Schechter mass function by [2] and [3]. We then use the same formalism to derive the double distribution for dark matter halos. We also discuss converting between linear and spherical-evolution density contrasts, and we present some interesting derivative quantities of the double distribution. In §III we explore the information content of our double-distribution by plotting the distribution itself as well as its derivative quantities for concordance ($\Omega_{\rm m} + \Omega_\Lambda = 1$) and Einstein-deSitter universes. Finally, we conclude and discuss our findings in §IV.

II. FORMALISM

A. Labeling of Cosmic Epochs

Throughout this paper we use the value of the dimensionless scale factor of the universe, a, to label different cosmic epochs. We normalize it so that the scale factor of the present is $a_0 = 1$. Then, a given value of a corresponds to a redshift

$$z = a^{-1} - 1\,, \tag{1}$$

independently of the cosmological model used. On the other hand, the conversion between a and time t does depend on the assumed cosmology. For a flat ($\Omega_{\rm tot} = \rho_{\rm tot}/\rho_{\rm c} = 1$) universe containing only matter and vacuum energy in the form of a cosmological constant (with present-day density parameters $\Omega_{\rm m} = \rho_{\rm m,0}/\rho_{\rm c,0}$ and $\Omega_\Lambda = \rho_{\Lambda,0}/\rho_{\rm c,0}$ respectively), the conversion equation is

$$t = \frac{2}{3} H_0^{-1} \Omega_\Lambda^{-1/2} \sinh^{-1}\left(\sqrt{a^3 \Omega_\Lambda/\Omega_{\rm m}}\right)\,, \tag{2}$$

where H_0 is the present-day value of the Hubble parameter. In the limiting case when $\Omega_\Lambda = 0$, $\Omega_{\rm m} = 1$, equation (2) becomes

$$t = \frac{2}{3} H_0^{-1} a^{3/2}\,. \tag{3}$$

We choose to cast our results in terms of a because it has a trivial and cosmology-independent relation with the directly observable redshift. In addition, it increases with time, which allows for a more intuitive interpretation of the evolution of the quantities we consider here.

B. Random Walks and the Press-Schechter Mass Function

The "random walk" formalism was introduced for the derivation of cosmological mass functions by [2] and by [3]. Here, we briefly review the basic concepts of this formalism, before extending it to the case of the double distribution in the next section.

The Press-Schechter mass function of collapsed structures is the comoving number density of virialized objects per differential mass interval, dn/dm, for every cosmic epoch a [32]. A related quantity is the mass fraction, $P(>m, a)$, which is the fraction of matter in the universe belonging to collapsed structures with mass $> m$. If $P(>m, a)$ is known, then dn/dm can be calculated from

$$\frac{dn}{dm}(m, a) = \frac{\rho_{\rm m,0}}{m}\left|\frac{d}{dm} P(>m, a)\right|\,, \tag{4}$$

where $\rho_{\rm m,0}$ is the present-day matter density of the universe.

$P(>m, a)$ is in turn calculated by assigning, at each epoch a, every infinitesimal element dm in the universe to a collapsed structure of some mass m. A structure is considered "collapsed" if its mean overdensity

$$\langle\delta\rangle = \frac{\langle\rho_{\rm structure}\rangle - \rho_{{\rm m},a}}{\rho_{{\rm m},a}} \tag{5}$$

exceeds a certain critical value, $\delta_{\rm c}(a)$. In equation (5), $\rho_{{\rm m},a}$ is the mean matter density of the universe at epoch a. The critical oversendity $\delta_{\rm c}(a)$ is the mean overdensity predicted by the spherical evolution model for a structure virializing at epoch a. For each point in space, one calculates the mean local overdensity by smoothing the overdensity field $\delta(\vec{x}, a)$ with a spherically symmetric filter function of varying mass scale, starting from $m \to \infty$, where one averages over the whole universe and finds identically $\langle\delta\rangle = 0$, and proceeding to successively smaller scales. When a mass scale is found for which the mean overdensity becomes equal to $\delta_{\rm c}(a)$, it is taken to be the mass m of the parent object of the infinitesimal mass at the point under consideration. This way of assigning object masses circumvents the structure-in-structure problem, since the mass of the parent object is always the *largest possible mass* satisfying the criterion

for collapse. All information on substructure within collapsed structures is thus erased from the resulting mass function.

The way the average overdensity $\langle\delta\rangle$ changes when the smoothing mass scale is varied resembles, under certain conditions, a 1D random walk [2]. For all "particles"(points in space in our case), the walk begins at the "spatial origin" ($\langle\delta\rangle = 0$), at "time zero" ($m \to \infty$). As "time progresses" (m decreases), each "particle" may move either to the "left" (negative $\langle\delta\rangle$) or to the "right" (positive $\langle\delta\rangle$). An "absorbing wall" exists at $\delta_{\rm c}(a)$. If this "wall" is reached, the "particle" is "removed" from the walk (the point is assigned its parent object mass and removed from further consideration at smaller values of m). $P(>m, a)$ is then the fraction of "particles" which have been "lost" by "time" m, and it can be calculated using random-walk theory.

However, we must first ensure that simple random-walk theory is indeed applicable. First, each "step" of the "walk" should be completely independent from the previous step. This requires that the k-modes producing an increase $\Delta\langle\delta\rangle$ in the space-like variable not appear in any of the previous steps in $\langle\delta\rangle$. A smoothing window function sharp in $k-$space,

$$\hat{W}_m(k) = \begin{cases} 1 & k < k_{\rm c}(m) \\ 0 & k > k_{\rm c}(m) \end{cases} \quad . \tag{6}$$

(see [2] and [3] for more extended discussions on the consequences of such a choice) enforces this condition, since

$$\langle\delta\rangle_{m,\vec{x}_0} = \int W_m\left(|\vec{x}_0 - \vec{x}|\right)\delta(\vec{x})d^3\vec{x} = \int_{k\le k_{\rm c}(m)} \delta_k {\rm e}^{i\vec{x}_0\cdot\vec{k}} d^3\vec{k} \tag{7}$$

and

$$\Delta\langle\delta\rangle_{\vec{x}_0} = \int_{k_{\rm c}(m)\le k\le k_{\rm c}(m-dm)} \delta_k {\rm e}^{i\vec{x}_0\cdot\vec{k}} d^3\vec{k} \tag{8}$$

which only involves new k-modes corresponding to scales from m to $m - dm$.

Second, there must be an equal probability for the system to "move" towards any one of the two available "directions". A Gaussian overdensity field (which is the usual assumption for deriving analytic mass functions and which we adopt in this paper) guarantees that this condition is satisfied.

Finally, the appropriate "time-like" variable (which should depend on m) needs to be selected, given that the "space-like" variable is $\langle\delta\rangle$. By direct analogy to the 1D random walk theory result $\langle x^2\rangle = 2Dt$, and from the definition of the variance of the overdensity field $S(m)$,

$$S(m) = \sigma^2(m) = \langle|\delta(m,\vec{x})|^2\rangle = \int_{k=0}^{k(m)} k^2 dk |\delta_k|^2 \tag{9}$$

we can immediately identify $Dt \to S(m)/2$.

Three further complications need to be addressed. First, our knowledge of δ_k and subsequently $S(m)$ is limited at late times. In the early universe, right after matter-radiation equality, $\langle|\delta_k|^2\rangle$ can be simply described in terms of a power-law in k modified by a transfer function, $\langle|\delta_k|^2\rangle \propto T^2(k)k^n$. While all δ are still in their linear regime, they simply grow by the linear growth factor (independent of k). However, at later times, when certain structures start departing from the linear regime, we cannot use our simple early-universe expressions for δ_k. Second, $\langle\delta\rangle$ is limited to be ≥ -1, which introduces a second, reflecting "wall" at a value of $\langle\delta\rangle = -1$, further complicating the random-walk calculations. Finally, the true overdensity field loses its Gaussianity as it evolves past the linear regime.

To circumvent these problems, we define the *linearly extrapolated overdensity field*, $\tilde{\delta}(\vec{x}, a)$, as the overdensity field that would result if all structures continued to grow according to the linear theory until time a. Now $\tilde{\delta}(\vec{x}, a)$ is not limited to be ≥ -1, since it does not represent real overdensities. In addition, we can always calculate $S(m)$ for $\tilde{\delta}(\vec{x}, a)$, since $\tilde{\delta}_k$ is modified from its simple early-universe expression only by the linear growth factor. Finally, the extrapolated field remains Gaussian at all times.

The linearly extrapolated overdensity $\tilde{\delta}(\vec{x}, a)$ and the associated variance $S(m)$, are time-varying, but the time dependence is well-known (see appendices B and C), and the same for both S and $\tilde{\delta}^2$ [33]. Thus, the time dependence drops out of ratios $\tilde{\delta}/\sqrt{S}$ which appear in the mass function. For this reason we may, without loss of generality, choose any single epoch to evaluate these quantities, with the stipulation that $\tilde{\delta}$ and $S(m)$ must refer to the same epoch. Given that $\sigma(m)$ is often normalized to the present value of σ_8, a convenient choice of epoch is the present. Then, equation (9) gives for $S(m)$

$$S(m) = \sigma_8^2 \frac{\int_{k=0}^{k(m)} T^2(k)k^{n+2}dk}{\int_{k=0}^{k(m_8)} T^2(k)k^{n+2}dk} \,. \tag{10}$$

Thus we only consider $\tilde{\delta}(\vec{x}, a_0)$ (the overdensity field linearly extrapolated to the present epoch), which we use instead of the true field $\delta(\vec{x}, a)$ in our random walk formalism [34]. To find the mass function at a particular cosmic epoch a, we calculate the location of the "absorbing wall", $\tilde{\delta}_{\rm c}(a)$. If a structure is predicted to collapse at epoch a according to the spherical evolution model, then $\tilde{\delta}_{0,{\rm c}}(a)$ is the overdensity this same structure would have had if, instead of turning around and collapsing, it had continued its linear evolution until the present. This $\tilde{\delta}_{0,{\rm c}}(a)$ is then our "absorbing wall".

We can now derive the mass fraction and mass function using random walk theory. If a particle executes a one-dimensional random walk with an absorbing boundary at a point x_1, then its probability $\mathcal{W}(x,t)$ to be between x and $x + dx$ at time t is [22]

$$\mathcal{W}(x,t,x_1)dx = \frac{\exp\left[-\frac{x^2}{4Dt}\right] - \exp\left[-\frac{(2x_1-x)^2}{4Dt}\right]}{2\sqrt{\pi Dt}} dx \,, \tag{11}$$

where $x \leq x_1$. In our case, the probability that a point in space will be assigned an average extrapolated overdensity between $\tilde{\delta}$ and $\tilde{\delta} + d\tilde{\delta}$ when filtered at a scale m corresponding to a variance of $S(m)$ is

$$\mathcal{W}(\tilde{\delta}, S, \tilde{\delta}_{0,\rm c}) d\tilde{\delta} = \frac{\exp\left[-\frac{\tilde{\delta}^2}{2S}\right] - \exp\left[-\frac{(2\tilde{\delta}_{0,\rm c} - \tilde{\delta})^2}{2S}\right]}{\sqrt{2\pi S}} d\tilde{\delta}\,, \tag{12}$$

with $\tilde{\delta} \leq \tilde{\delta}_{0,\rm c}$. The mass fraction $P(>m, a)$ is then the fraction of points already "lost" from the walk when filtering at higher mass scales, which is one minus the fraction of points remaining in the walk,

$$\begin{aligned} P(>m, a) &= P(>\tilde{\delta}_{0,\rm c}) = 1 - \int_{-\infty}^{\tilde{\delta}_{0,\rm c}} \mathcal{W}(\tilde{\delta}, S, \tilde{\delta}_{0,\rm c}) d\tilde{\delta} \\ &= \mathrm{erfc}\left(\frac{\tilde{\delta}_{0,\rm c}(a)}{\sqrt{2S(m)}}\right). \end{aligned} \tag{13}$$

Then,

$$\frac{dP(>m, a)}{dm} = \frac{1}{\sqrt{2\pi}} \frac{\tilde{\delta}_{0,\rm c}(a)}{S(m)^{3/2}} \frac{dS}{dm} \exp\left[-\frac{\tilde{\delta}_{0,\rm c}(a)^2}{2S(m)}\right], \tag{14}$$

and the Press-Schechter mass function can be found using equation (4),

$$\frac{dn}{dm}(m, a) = \sqrt{\frac{2}{\pi}} \frac{\rho_{\rm m,0}}{m^2} \frac{\tilde{\delta}_{0,\rm c}(a)}{\sqrt{S(m)}} \left|\frac{d\ln\sqrt{S}}{d\ln m}\right| \exp\left[-\frac{\tilde{\delta}_{0,\rm c}(a)^2}{2S(m)}\right]. \tag{15}$$

C. Derivation of the Double Distribution

We now use the random walk formalism described in the previous section to derive the double distribution of the comoving number density of collapsed structures with respect to object mass m and local environment overdensity δ_ℓ, $dn/(dm\, d\delta_\ell)$.

For the reasons described in the previous section, we replace the true overdensity field, $\delta(\vec{x}, a)$, with its linear extrapolation to the present time, $\tilde{\delta}(\vec{x}, a_0)$. Thus, we derive the double distribution of comoving n with respect to object mass m and *extrapolated* local environment overdensity $\tilde{\delta}_\ell$, $dn/(dm\, d\tilde{\delta}_\ell)$. We then use linear theory and the spherical evolution model to establish a conversion relation $\delta(\tilde{\delta}, a)$ and calculate $dn/(dm\, d\delta_\ell)$ as

$$\frac{dn}{dm d\delta_\ell}(\delta_\ell, m, a) dm d\delta_\ell = \frac{dn}{dm d\tilde{\delta}_\ell}\left[\tilde{\delta}_\ell(\delta_\ell, a), m, a\right] dm \frac{\partial\tilde{\delta}}{\partial\delta_\ell} d\delta_\ell\,. \tag{16}$$

First of all, we need to define the local environment extrapolated overdensity $\tilde{\delta}_\ell$ in a precise way. We would like $\tilde{\delta}_\ell$ to be a measure of the density contrast of the medium in which a collapsed structure is embedded. Clearly, the value of $\tilde{\delta}_\ell$ depends on how far from the structure itself its "environment" extends. We quantify this notion by introducing the **clustering scale parameter**, β, which is defined in the following way: the "environment" of an object of mass m is a surrounding region in space which encompasses mass βm (including the mass of the object). Hence, the local environment extrapolated overdensity $\tilde{\delta}_\ell$ is the result of a filtering of $\tilde{\delta}(\vec{x}, a_0)$ with a filter of scale βm centered on the object.

Formally, the above definition translates as follows. Consider the sharp in $k-$space filtering function $\hat{W}_m(k)$ discussed previously (eq. 6). The relation between the cutoff wavenumber and the filter mass, $k_{\rm c}(m)$, is found by considering the form of the filter function in configuration space,

$$W_m(r) = \frac{\sin\left[k_{\rm c}(m)r\right] - k_{\rm c}(m)r\cos\left[k_{\rm c}(m)r\right]}{2\pi^2 r^3}, \tag{17}$$

and multiplying by $\rho_{\rm m,0}$ and integrating over all space, which yields [3],

$$k_{\rm c}(m) = \left(\frac{6\pi^2\rho_{\rm m,0}}{m}\right)^{1/3}. \tag{18}$$

For a collapsed structure at an epoch a which has mass m and is centered at a point $\vec{x}_0$, we can write

$$\tilde{\delta}(m, \vec{x_0}) = \int W_m\left(|\vec{x}_0 - \vec{x}|\right) \tilde{\delta}(\vec{x}, a_0) d^3\vec{x} = \tilde{\delta}_{0,\rm c}(a)\,, \tag{19}$$

since the mean extrapolated overdensity of the collapsed structure itself is always the critical value for collapse, $\tilde{\delta}_{0,\rm c}(a)$. For that same object, the *local environment extrapolated overdensity*, $\tilde{\delta}_\ell$, is

$$\tilde{\delta}_\ell(m, \vec{x_0}) = \int W_{\beta m}\left(|\vec{x}_0 - \vec{x}|\right) \tilde{\delta}(\vec{x}, a_0) d^3\vec{x}\,. \tag{20}$$

Equation (20) is then the definition of $\tilde{\delta}_\ell$ for a given β. In our double distribution, β is free parameter, which is however constrained to be between 1 and a few on physical grounds. It cannot be < 1 since the mass of the object's environment always includes the mass of the object itself. In fact, as β approaches 1, the averaging which produces $\tilde{\delta}_\ell$ is taken *only* over the collapsed object itself, and inevitably returns the critical overdensity for collapse, $\tilde{\delta}_{0,\rm c}$, for all objects. In the other extreme, $\beta \gg 1$, the average $\tilde{\delta}$ on a scale βm is no longer a local quantity with respect to the central object. When β grows without bound, $\tilde{\delta}_\ell$ approaches 0 for all collapsed structures, since averaging over the whole universe identically returns the background matter density, which corresponds to a vanishing density contrast. In appendix A we show that our double distribution becomes proportional to a Dirac delta-function around $\tilde{\delta}_\ell = 0$ in the limit $\beta \to \infty$ and proportional to a Dirac delta-function around $\tilde{\delta}_\ell = \tilde{\delta}_{0,\rm c}$ in the limit $\beta \to 1$.

We are now ready to use random walk theory results to calculate the double distribution. We first find the fraction of points in space which belong to structures of

mass between m and $m+dm$, which in turn are embedded in a medium of mean linearly extrapolated overdensity between $\tilde{\delta}_\ell$ and $\tilde{\delta}_\ell + d\tilde{\delta}_\ell$, $f(m,\tilde{\delta}_\ell,\beta)d\tilde{\delta}_\ell\, dm$. The double distribution then is

$$\frac{dn}{dmd\tilde{\delta}_\ell} = \frac{\rho_{\rm m,0}}{m} f(m,\tilde{\delta}_\ell,\beta)dmd\tilde{\delta}_\ell. \quad (21)$$

The quantity f can be written as

$$f dm\, d\tilde{\delta}_\ell = (f_1 d\tilde{\delta}_\ell)(f_2 dm) \quad (22)$$

where $f_1 d\tilde{\delta}_\ell$ is the fraction of points in space which have an average overdensity between $\tilde{\delta}_\ell$ and $\tilde{\delta}_\ell + d\tilde{\delta}_\ell$ on a smoothing scale βm, and $f_2 dm$ is the fraction of points satisfying the previous condition which belong to collapsed structures of mass between m and $m+dm$.

The first of the two factors above is the fraction of points still in the walk which are found between $\tilde{\delta}$ and $\tilde{\delta}+d\tilde{\delta}$ at a "time" βm. This is the solution of the 1D random walk problem of $\tilde{\delta}_\ell$ as a function of S, with an absorbing boundary at the critical collapse threshold $\tilde{\delta}_{0,\rm c}$, as given by equation (12) but for a smoothing scale βm,

$$f_1 d\tilde{\delta}_\ell = \frac{\exp\left[-\frac{\tilde{\delta}_\ell^2}{2S(\beta m)}\right] - \exp\left[\frac{(\tilde{\delta}_\ell - 2\tilde{\delta}_{0,\rm c}(a))^2}{2S(\beta m)}\right]}{\sqrt{2\pi S(\beta m)}} d\tilde{\delta}\,. \quad (23)$$

The second factor (f_2) is the *conditional probability* that a point in space originating from $(\beta m, \tilde{\delta})$ in the mass - overdensity plane,will reach the "wall" for the first time for a smoothing scale between m and $m+dm$. This is then the probability that a particular point in space is absorbed by the "wall" $\tilde{\delta}_{0,\rm c}(a)$ at a particular "time" $S(m)$, provided that the origin of the walk is transferred from $(0,0)$ to $(S(\beta m),\tilde{\delta}_\ell)$. This probablility can then be found if, in the expression for $dP(>m,a)/dm$ (eq. 14), we perform the substitutions $\tilde{\delta}_{0,\rm c} \to \tilde{\delta}_{0,\rm c} - \tilde{\delta}_\ell$ and $S(m) \to S(m) - S(\beta m)$. Similar conditional probabilities were originally calculated by [2] and [3] in the context of rates of mergers between halos. In our case, it is

$$f_2 dm = \frac{\left[\tilde{\delta}_{0,\rm c}(a) - \tilde{\delta}_\ell\right] \exp\left[-\frac{\left(\tilde{\delta}_{0,\rm c}(a)-\tilde{\delta}_\ell\right)^2}{2[S(m)-S(\beta m)]}\right]}{\sqrt{2\pi}\left[S(m)-S(\beta m)\right]^{3/2}} \left|\frac{dS}{dm}\right|_m dm\,. \quad (24)$$

Equations (21) and (22) then give

$$\frac{dn}{dmd\tilde{\delta}_\ell}(m,\tilde{\delta}_\ell,\beta,a) = \frac{\rho_{\rm m,0}}{m}\,\frac{\tilde{\delta}_{0,\rm c}(a)-\tilde{\delta}_\ell}{2\pi}\,\frac{\exp\left[-\frac{\tilde{\delta}_\ell^2}{2S(\beta m)}\right] - \exp\left[-\frac{\left(\tilde{\delta}_\ell - 2\tilde{\delta}_{0,\rm c}(a)\right)^2}{2S(\beta m)}\right]}{[S(\beta m)]^{1/2}\left[S(m)-S(\beta m)\right]^{3/2}} \left|\frac{dS}{dm}\right|_m \exp\left[-\frac{\left(\tilde{\delta}_{0,\rm c}(a)-\tilde{\delta}_\ell\right)^2}{2\left[S(m)-S(\beta m)\right]}\right] \quad (25)$$

with $\tilde{\delta}_\ell \le \tilde{\delta}_{0,\rm c}(a)$ and $\beta > 1$ so $S(m) > S(\beta m)$ [35]. Equation (25) is the double distribution we have sought and is the central result of this paper. Integrating $dn/(dmd\tilde{\delta}_\ell)$ over $\tilde{\delta}_\ell$ yields the Press-Schechter mass function, as it should. The result is independent of the value of β. We explicitly perform this integration in appendix A.

Note that the functional form of our double distribution is similar with that of the integrand used by [13] in their calculation of the cross-correlation between dark halos and mass using random walk theory, however the second variance of the field (corresponding to our $S(\beta m)$) in their case refers to a fixed clustering radius and is independent of object mass.

D. Converting between $\tilde{\delta}_\ell$ and δ_ℓ

In appendices B and C we derive exact expressions for $\tilde{\delta}_\ell(\delta_\ell, a)$ in the case of the spherical evolution model, for an $\Omega_{\rm m} = 1$ (appendix B) and an $\Omega_{\rm m} + \Omega_\Lambda = 1$ (appendix C) universe (note however that all of the equations we have presented up to this point are cosmology-independent, and can therefore be adapted for any cosmological model).

An excellent approximation to these conversion relations can be derived from the expression

$$\tilde{\delta}_a \approx \tilde{\delta}_{\rm c}\left[1 - (1+\delta_a)^{-1/\tilde{\delta}_{\rm c}}\right]. \quad (26)$$

Similar approximations were suggested by [23] and [15]. Equation (26) relates the linear overdensity at a time a to the true overdensity at the same time, and its accuracy is *better than 2% throughout its domain* for both $\Omega_{\rm m} = 1$ and $\Omega_{\rm m} + \Omega_\Lambda = 1$ cosmologies. Its functional form is much simpler and more intuitive than the more accurate fit of [13]. The cosmological model enters only through $\tilde{\delta}_{\rm c}$. For the Einstein-deSitter universe, $\tilde{\delta}_{\rm c}$ is given by equation (B17) for $a_{\rm coll} = 1$, while for the $\Omega_{\rm m} + \Omega_\Lambda = 1$ universe it is given by equation C29 for $a = 1$. Note that $\tilde{\delta}_{\rm c}$ is related to the quantity $\tilde{\delta}_{0,\rm c}(a)$ (which appears explicitly in our double distribution expression) through

$$\tilde{\delta}_{0,\rm c}(a) = \tilde{\delta}_{\rm c}\frac{D(a_0)}{D(a)} \quad (27)$$

where $D(a)$ is the linear growth factor in the relevant cosmology.

The limits of equation (26) are the same as the ones required for the exact conversion relation. When $|\delta_a| \ll 1$, $\tilde{\delta}_a \approx \delta_a$. In addition, $\tilde{\delta}_a \to -\infty$ as $\delta_a \to -1$, and $\delta_a \to \infty$ as $\tilde{\delta}_a \to \tilde{\delta}_c$.

Using equation (26),

$$\tilde{\delta}_\ell \approx \frac{D(a_0)}{D(a)}\tilde{\delta}_c \left[1 - (1+\delta_\ell)^{-1/\tilde{\delta}_c}\right], \qquad (28)$$

where a is the time at which we want to evaluate the double distribution. Note that close to virialization, equation (28) loses its applicability (as does the spherical collapse model), and has to be replaced by a recipe which does not diverge in δ. We present such recipes in appendices B and C, however the exact functional form of the conversion relation in this regime cannot affect any of the physically interesting results as the amplitude of the double distribution decreases rapidly enough with δ that the contribution of the high-delta tail to the integrated mass function is negligible. We have verified this fact by comparing the integral of our double distribution over δ with the Press-Schechter mass function. When we extended the integration up to δ_c, the results agreed to the accuracy of the numerical integration. When we extended our integration only up to δ_v (just below the application of our virialization recipe), the error relative to the Press-Schechter mass function was less than 0.02%.

E. Clustering Scale Lengths and Correction for Central Object Contamination

The definition of β and $\tilde{\delta}_\ell$ described above was sufficient for us to derive the double distribution from random walk theory. However, from a physical point of view, the presence of a collapsed structure at the center of the "environment sphere" contaminates the evaluation of the average "environmental" overdensity. If we want the double distribution to describe the properties of matter *surrounding* collapsed objects, we need to correct for the presence of the objects themselves.

We will employ a simple, "top-hat" physical picture to calculate an appropriate correction (see also [15]). Note however that our correction is approximate, since the filter we used to smooth the overdensity field was $k-$sharp rather than top-hat in space.

Let δ_c be the (true) overdensity of a collapsed object of mass m and radius R_v, and δ_ℓ be the overdensity of the "environment sphere" of radius R_e. The "environment sphere" encompasses a mass βm, including the central collapsed object. We want to find the average overdensity δ_{ext} of that part of the "environment sphere" which is *external* to the central object. For the collapsed object we can write

$$m = \frac{4}{3}\pi R_v^3 (1+\delta_c)\rho_m\,, \qquad (29)$$

where ρ_m is the mean matter density of the universe at the epoch of interest. For the environment sphere, including the central object, we can write

$$\beta m = \frac{4}{3}\pi R_e^3 (1+\delta_\ell)\rho_m\,. \qquad (30)$$

From equations (29) and (30) we get $R_v^3 = R_e^3(1+\delta_\ell)/\beta(1+\delta_c)$. It thus follows that the length scale R_e associated with the clustering parameter β is

$$\begin{aligned} R_e &= \left(\frac{\beta(1+\delta_c)}{1+\delta_\ell}\right)^{1/3} R_v \\ &= \left(\frac{3\beta m}{4\pi(1+\delta_\ell)\rho_m}\right)^{1/3}. \end{aligned} \qquad (31)$$

We see that for a fixed clustering parameter β, the length scale associated with an object of mass m is mass-dependent, scaling linearly with the virial radius but larger by a factor $[\beta(1+\delta_c)/(1+\delta_\ell)]^{1/3} > 1$. Thus, we can roughly think of the clustering scale parameter as a measure of how many virial radii we include as the local environment around each structure [36].

Having identified the environmental length scale, we can now isolate the environmental overdensity from that of the collapsed object. The volume of the environment sphere external to the central object contains a mass

$$(\beta-1)m = \frac{4}{3}\pi(R_e^3 - R_v^3)(1+\delta_{ext})\rho_m\,. \qquad (32)$$

Using equation (31) to eliminate R_v, and dividing by equation (30) we obtain

$$\delta_{ext} = \frac{(\beta-1)(1+\delta_\ell)(1+\delta_c)}{\beta(1+\delta_c) - (1+\delta_\ell)} - 1\,, \qquad (33)$$

which is the contamination-corrected overdensity for an environment sphere with uncorrected overdensity δ_ℓ. Then, the contamination-corrected double distribution will be given by

$$\frac{dn}{dm d\delta_{ext}}(\delta_{ext}, m, a) = \frac{dn}{dm d\delta_\ell}\left[\delta_\ell(\delta_{ext}, a), m, a\right]\frac{d\delta_\ell}{d\delta_{ext}}\,, \qquad (34)$$

where

$$\delta_\ell(\delta_{ext}) = \frac{\beta(1+\delta_{ext})(1+\delta_c)}{(\beta-1)(1+\delta_c) + (1+\delta_{ext})} - 1 \qquad (35)$$

and

$$\frac{d\delta_\ell}{d\delta_{ext}} = \frac{\beta(\beta-1)(1+\delta_c)^2}{\left[(\beta-1)(1+\delta_c) + (1+\delta_{ext})\right]^2}\,. \qquad (36)$$

F. Derivative Quantities

We now have enough tools to calculate derivative quantities of interest. The number density of collapsed objects

of mass greater than some minimum $m_{\rm min}$ [37] embedded in a medium of local overdensity between $\delta_{\rm ext}$ and $\delta_{\rm ext} + d\delta_{\rm ext}$ is

$$\frac{dn}{d\delta_{\rm ext}}(> m_{\rm min})d\delta_{\rm ext} = d\delta_{\rm ext}\frac{\partial\tilde{\delta}_\ell}{\partial\delta_\ell}\frac{d\delta_\ell}{d\delta_{\rm ext}}\int_{m=m_{\rm min}}^{\infty}\frac{dn}{dmd\tilde{\delta}_\ell}dm\,, \tag{37}$$

while the density of matter in collapsed objects of mass $> m_{\rm min}$ embedded in a medium of local overdensity between $\delta_{\rm ext}$ and $\delta_{\rm ext} + d\delta_{\rm ext}$ is

$$\frac{d\rho}{d\delta_{\rm ext}}(> m_{\rm min})d\delta_{\rm ext} = d\delta_{\rm ext}\frac{\partial\tilde{\delta}_\ell}{\partial\delta_\ell}\frac{d\delta_\ell}{d\delta_{\rm ext}}\int_{m=m_{\rm min}}^{\infty} m\frac{dn}{dmd\tilde{\delta}_\ell}dm\,. \tag{38}$$

Of all the matter in the universe which belongs to collapsed objects of mass $> m_{\rm min}$, the fraction by mass which lives in underdense neighborhoods is

$$f_{\rho,{\rm un}} = \frac{\int_{\delta_{\rm ext}=-1}^{0}\frac{d\rho}{d\delta_{\rm ext}}(> m_{\rm min})d\delta_{\rm ext}}{\int_{\delta_{\rm ext}=-1}^{\delta_{\rm c}}\frac{d\rho}{d\delta_{\rm ext}}(> m_{\rm min})d\delta_{\rm ext}}\,. \tag{39}$$

Then, the mass fraction of the matter defined above which lives in overdensities will be $f_{\rho,{\rm ov}} = 1 - f_{\rho,{\rm un}}$.

Similarly, of all the objects with mass $m > m_{\rm min}$, a fraction by number which lives inside underdensities is

$$f_{\rm n,un} = \frac{\int_{\delta_{\rm ext}=-1}^{0}\frac{dn}{d\delta_{\rm ext}}(> m_{\rm min})d\delta_{\rm ext}}{\int_{\delta_{\rm ext}=-1}^{\delta_{\rm c}}\frac{dn}{d\delta_{\rm ext}}(> m_{\rm min})d\delta_{\rm ext}}\,. \tag{40}$$

The complementary number fraction of such structures living inside overdensities will be $f_{\rm n,ov} = 1 - f_{\rm n,un}$.

The number-density–weighted mean $\delta_{\rm ext}$ for structures of mass $> m_{\rm min}$ is

$$\langle\delta\rangle_{\rm n} = \frac{\int_{\delta_{\rm ext}=-1}^{\delta_{\rm c}}\delta_{\rm ext}\frac{dn}{d\delta_{\rm ext}}(> m_{\rm min})d\delta_{\rm ext}}{\int_{\delta_{\rm ext}=-1}^{\delta_{\rm c}}\frac{dn}{d\delta_{\rm ext}}(> m_{\rm min})d\delta_{\rm ext}} \tag{41}$$

with a variance

$$\sigma^2_{\delta,{\rm n}} = \frac{\int_{\delta_{\rm ext}=-1}^{\delta_{\rm c}}(\delta_{\rm ext} - \langle\delta\rangle_{\rm n})^2\frac{dn}{d\delta_{\rm ext}}(> m_{\rm min})d\delta_{\rm ext}}{\int_{\delta_{\rm ext}=-1}^{\delta_{\rm c}}\frac{dn}{d\delta_{\rm ext}}(> m_{\rm min})d\delta_{\rm ext}}\,. \tag{42}$$

Similarly, the matter-density–weighted mean δ for structures of mass $> m_{\rm min}$ is

$$\langle\delta\rangle_{\rho} = \frac{\int_{\delta_{\rm ext}=-1}^{\delta_{\rm c}}\delta_{\rm ext}\frac{d\rho}{d\delta_{\rm ext}}(> m_{\rm min})d\delta_{\rm ext}}{\int_{\delta_{\rm ext}=-1}^{\delta_{\rm c}}\frac{d\rho}{d\delta_{\rm ext}}(> m_{\rm min})d\delta_{\rm ext}} \tag{43}$$

with a variance

$$\sigma^2_{\delta,\rho} = \frac{\int_{\delta_{\rm ext}=-1}^{\delta_{\rm c}}(\delta_{\rm ext} - \langle\delta\rangle_{\rho})^2\frac{d\rho}{d\delta_{\rm ext}}(> m_{\rm min})d\delta_{\rm ext}}{\int_{\delta_{\rm ext}=-1}^{\delta_{\rm c}}\frac{d\rho}{d\delta_{\rm ext}}(> m_{\rm min})d\delta_{\rm ext}}\,. \tag{44}$$

III. RESULTS

In this section we present plots of the double distribution itself as well as of its various physically interesting derivative quantities. We compare results derived for a concordance, $\Omega_{\rm m} + \Omega_\Lambda = 1$ universe with WMAP parameters ($\sigma_8 = 0.84$, $h = 0.71$, $\Omega_{\rm m} = 0.27$, $\Omega_{\rm b} = 0.04$, [24]), and for an Einstein-deSitter ($\Omega_{\rm m} = 1$) universe with $h = 0.71$, $\Omega_{\rm b} = 0.04$, but $\sigma_8 = 0.45$. The different power-spectrum normalization in the Einstein-deSitter case was selected so that the Press-Schechter mass function in this case coincides with that of the concordance universe on a mass scale of $5.5 \times 10^{14}{\rm M}_\odot$, which is between the values of m_8 (mass included in a sphere of comoving radius $8h^{-1}$ Mpc) for the two cosmologies ($m_8 = 2 \times 10^{14}\,{\rm M}_\odot$ for the concordance universe while $m_8 = 8 \times 10^{14}\,{\rm M}_\odot$ for the Einstein-de Sitter universe). This value of σ_8 is also consistent with the fits of [9] given the WMAP result for the concordance universe. Finally, we use fitting formulae of [25] for the adiabatic cold dark matter transfer function to calculate the density field variance $S(m)$. In this section, δ always refers to $\delta_{\rm ext}$, the true overdensity of that part of the "environment sphere" which is external to the central object.

Figure 1 shows a 3-dimensional rendering of our double distribution as a function of mass and overdensity for fixed $\beta = 2$ and $z = 0$. The left panel corresponds to the concordance universe while the right panel corresponds to the Einstein-deSitter universe, and this arrangement is retained throughout this section.

The features of the double distribution are demonstrated in more quantitative detail in Figures 2-5. Figures 2 and 3 show slices of the double distribution at constant values of mass. In Figure 2, different curves correspond to different values of the central object mass. In Fugure 3, all curves are for an object mass $m = 5.5 \times 10^{15}\,{\rm M}_\odot$, and different curves correspond to different redshifts. Their most prominent feature is the pronounced peak at a relatively low value of $|\delta|$, indicating that for each given pair of z and m, there is a preferred, "most probable" value of the local environment density contrast. As we can see in Figure 2, the location of this peak moves to higher values of the density contrast as the mass of the object increases: small structures are preferentially located in relative isolation, while larger structures are more likely to be found in clustered environments. This result fits well in the picture of hierarchical structure formation, as smaller structures tend to be merged into higher-mass objects as time progresses. Lower-mass objects which are initially part of underdensities are less probable to undergo mergers, and hence are more likely to survive at late times than objects which are initially part of overdensities. Conversely, higher-mass structures are more likely to be parts of overdensities where they can accumulate mass more easily through mergers with smaller structures.

Note, however, that in the hierarchical structure formation picture, the mass scale where the exponential

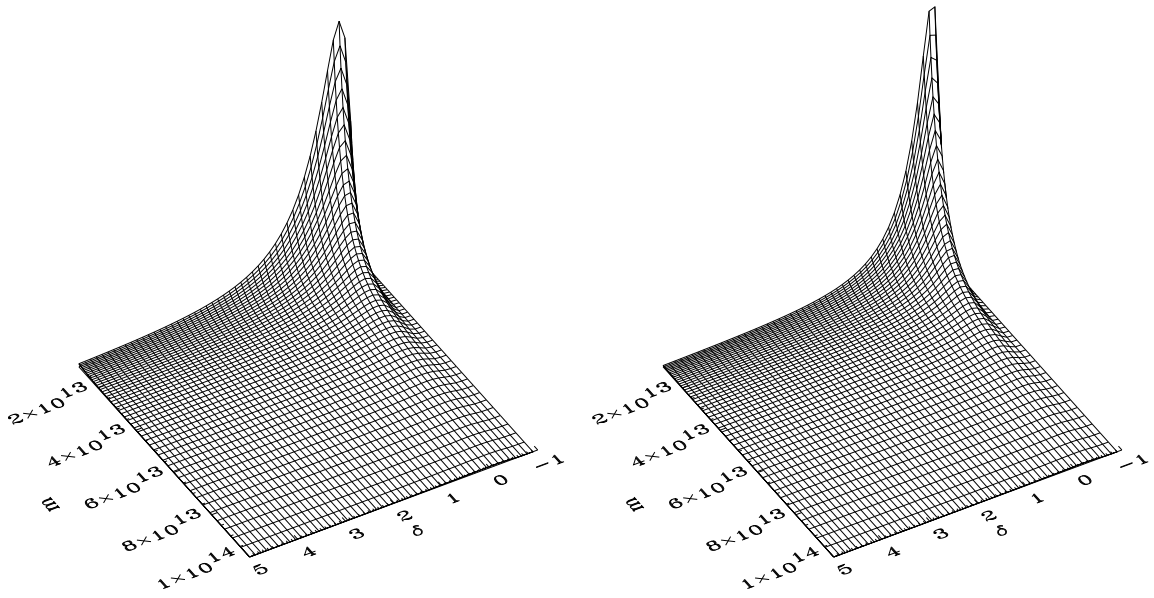

FIG. 1: Surface plots of the double distribution for $z = 0$ and $\beta = 2$ in $\Omega_{\rm m} + \Omega_\Lambda = 1$ (left panel) and Einstein-deSitter (right panel) universes. The mass is measured in $\mathrm{M}_\odot$. The vertical axis is linear, with the $m - \delta$ axes level corresponding to $dn/dmd\delta_\ell = 0$ and the highest point corresponding to $dn/dmd\delta_\ell = 2.72 \times 10^{-2}$ (left panel) and $dn/dmd\delta_\ell = 1.89 \times 10^{-1}$ (right panel) objects per Mpc^3 per $10^{15}\mathrm{M}_\odot$.

suppression of collapsed structures sets in increases with time. Thus, any given mass scale starts out as being a "high mass" at early times and eventually becomes a "lower mass" as it enters the power-law regime of the Press-Schechter mass function. Hence, according to the argument we used to explain Figure 2, the double distribution for any given mass scale should peak at increasing δ values with increasing redshift. This is because a particular mass scale used to be closer to the high-mass end of the halo distribution in the past than it is today. Indeed, this is the trend seen in Figure 3. As we would expect, the peak of the distribution moves to higher δ values with increasing redshift. The significantly more pronounced suppression of this mass scale in high redshifts in the Einstein-deSitter universe is due to the different power-spectrum normalization in the two cosmological models. Because of our choice in the power-spectrum normalization, the exponential suppression in the number density of structures sets in at lower masses in the Einstein-de Sitter case than in the concordance universe. Thus, there is a tendency to see more structures of higher mass in our concordance results than in the Einstein-de Sitter case, despite the intuitive expectation that a higher $\Omega_{\rm m}$ universe should have more massive structures at late times due to its ability to continue to form structures even at the present epoch. This would indeed have been the case if the power-spectrum had been normalized in the same way.

That halos of a given mass are more strongly clustered with increasing redshift was also found by [26], who used $\Delta_8(m)$ (the rms overdensity in the number of haloes more massive than some mass scale after smoothing with a spherical top-hat filter of comoving radius $8h^{-1}$ Mpc) as a measure for halo clustering. A tendency of higher mass objects to be found in overdense regions was discussed by [13] and [12], who interpreted it by viewing halos today as progenitors of future larger-scale structures viewed at "high" or "low" redshift.

In addition to the main peak at low $|\delta|$, an additional, much lower and sharper peak can be seen right before the critical overdensity cutoff. This peak is the result of the change of the functional form of the conversion relation between linearly extrapolated and true density contrast close to virialization, when application of the spherical collapse morel would lead δ to diverge. The particular shape of the peak is an artifact of the recipe we adopted for dealing with the virialization regime, and carries no physical meaning (the shape of the peak is the shape of the high-δ end of $d\tilde{\delta}/d\delta$). However, since the boundary conditions we use for $\tilde{\delta}(\delta)$ and its derivative *are* physical, we do expect to have some form of local maximum at the high-δ end of the double distribution. Still, as discussed in the previous section, the effect of the details or even the existence of this local maximum on the physical quantities of interest is negligible.

The high-δ cutoff occurs at higher values of δ in the concordance universe than in the Einstein-deSitter universe. This is a result of the different density contrast

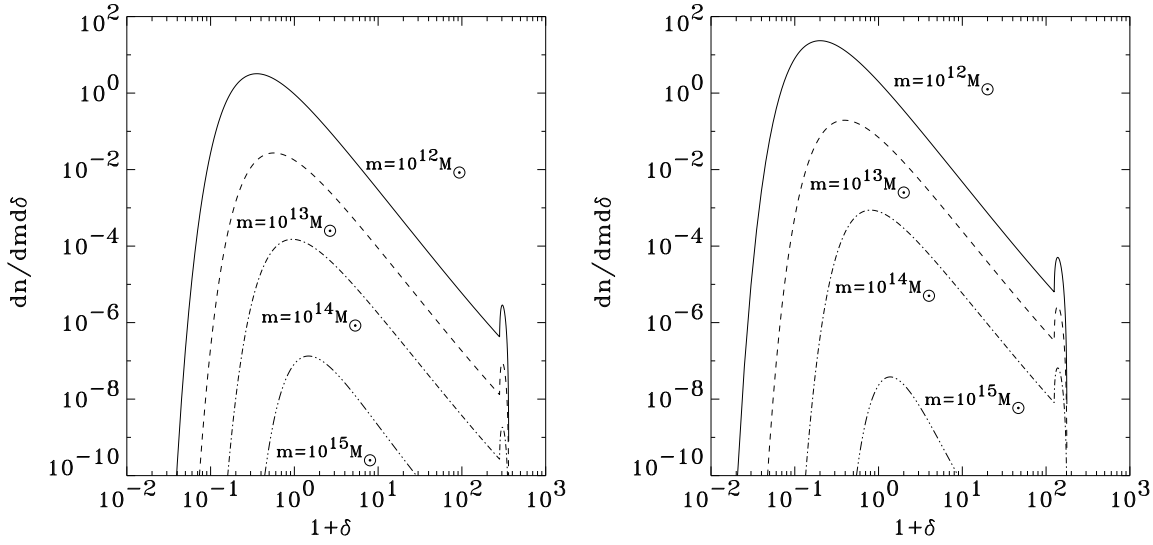

FIG. 2: Slices of the double distribution function at various fixed values of the mass for $\Omega_{\rm m} + \Omega_\Lambda = 1$ (left panel) and Einstein-deSitter (right panel) universes. The units of the double distribution are number of objects per Mpc^3 per $10^{15}\mathrm{M}_\odot$.

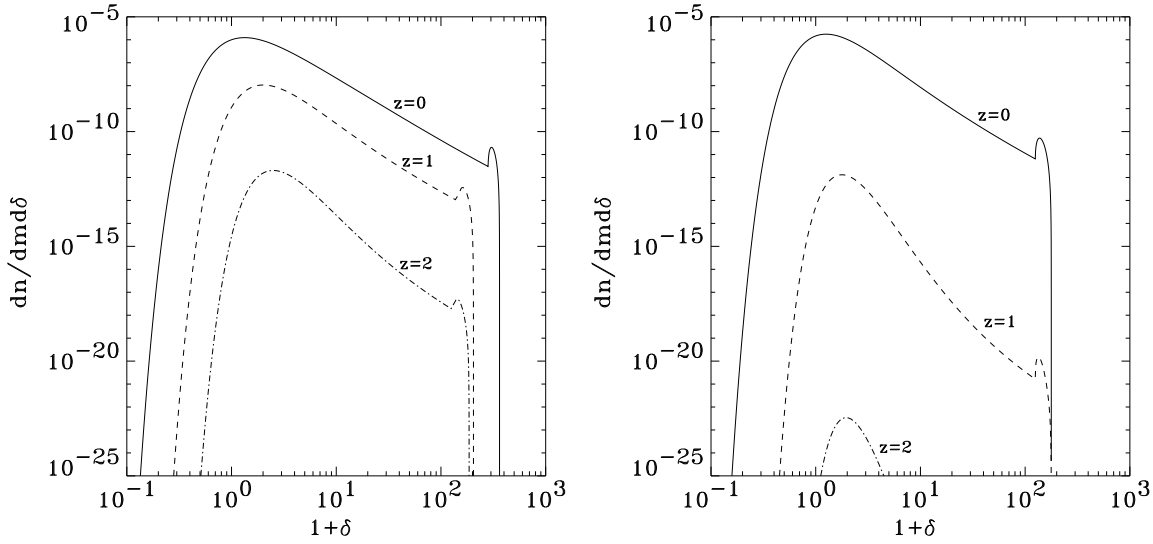

FIG. 3: Slices of the double distribution function at $m = 5.5 \times 10^{14}, \mathrm{M}_\odot$ and for various values of redshift z, for $\Omega_{\rm m} + \Omega_\Lambda = 1$ (left panel) and Einstein-deSitter (right panel) universes. The units of the double distribution are number of objects per Mpc^3 per $10^{15}\mathrm{M}_\odot$.

achieved at virialization by structures in the two different cosmologies. In the Einstein-deSitter case this density contrast is always $18\pi^2$, while in the concordance universe it is always higher and increases with time. At high redshifts, before the effect of Λ becomes significant, $\delta_{\rm c}$ is very close to $18\pi^2$ in the concordance universe as well, as can be seen in Figure 3.

Figures 4 and 5 show slices of the double distribution at various fixed values of δ, with $z = 0$ and $\beta = 2$. Figure 4 plots slices corresponding to relatively low values of $|\delta|$ ($\delta = -0.5, 0, 0.5$ and 3, close to the distribution peak in δ). At the high-mass end of the distribution, the abundance of objects increases with increasing δ, while in the low mass end of the distribution the trend is reversed, and the object abundance increases with decreasing δ. This is in agreement with the behavior observed in the constant-m slices.

Figure 5 plots slices corresponding to high values of δ ($\delta = 10, 20$ and 30), farther from the distribution peack. In this case, the curves do not cross, and an increase of δ simply results in an overall suppression of object abundance: structures of all masses are unlikely to be found

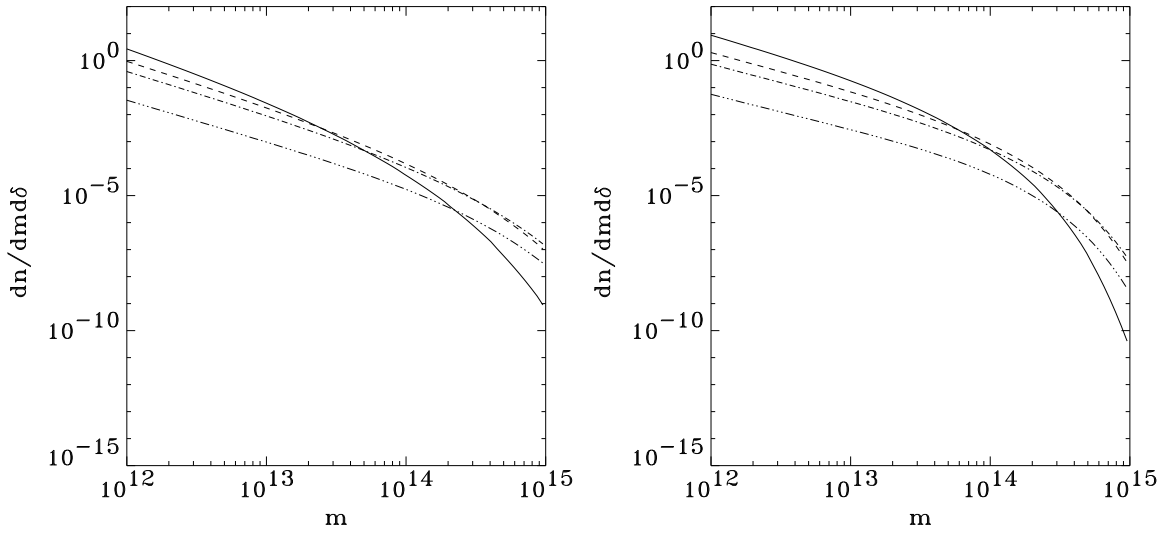

FIG. 4: Slices of the double distribution function at constant values of δ for $z = 0$, $\beta = 2$ and for $\Omega_{\rm m} + \Omega_\Lambda = 1$ (left panel) and Einstein-deSitter (right panel) universes. Solid line: $\delta = -0.5$; dashed line: $\delta = 0$; dot-dashed line: $\delta = 0.5$; double-dot–dashed line: $\delta = 3$. The units of the double distribution are number of objects per Mpc^3 per 10^{15}M$_\odot$.

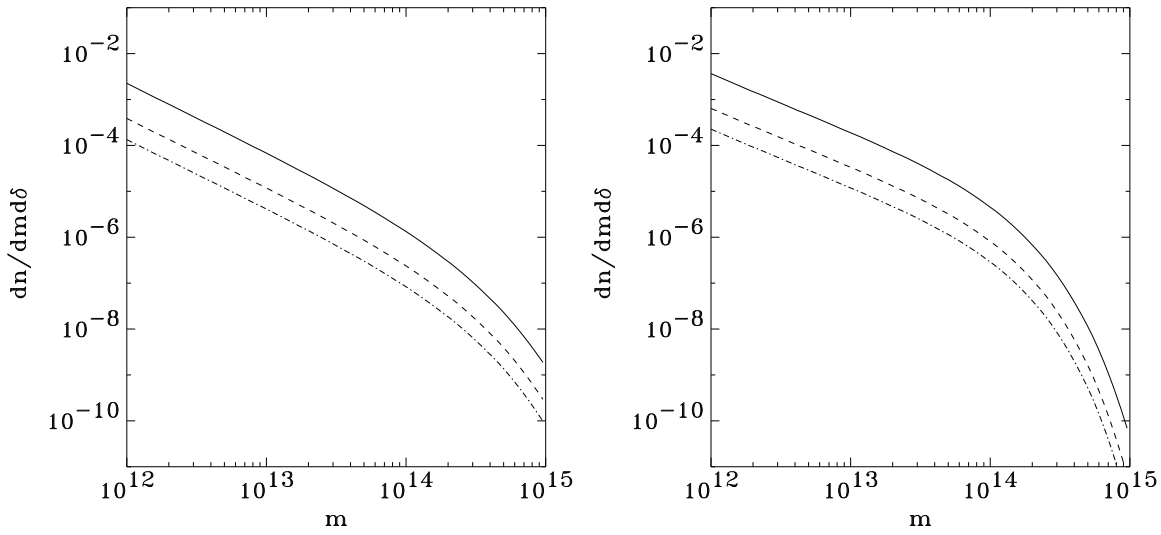

FIG. 5: Slices of the double distribution function at constant values of δ for $z = 0$, $\beta = 2$, and for $\Omega_{\rm m} + \Omega_\Lambda = 1$ (left panel) and Einstein-deSitter (right panel) universes. Solid line: $\delta = 10$; dashed line: $\delta = 20$; dot-dashed line: $\delta = 30$. The units of the double distribution are number of objects per Mpc^3 per 10^{15}M$_\odot$.

overly clustered. This is because the final stages of collapse proceed rather quickly compared to the time spent around turnaround. The likelihood of a region observed in its late stages of collapse but before virialization is then low because the lifetime of this phase is small.

In figure 6 we plot $dn/d\delta(> 10^{12}{\rm M}_\odot)$ as a function of $1 + \delta$ for different values of redshift. It is striking that at $z = 0$, the distribution peaks at negative δ values (around $\delta = -0.6$ in the concordance and -0.7 in the Einstein-deSitter universe), indicating that the most probable location for a collapsed object of mass $> 10^{12}\,{\rm M}_\odot$ is an *underdense* environment. For the specific mass range, this trend is reversed by $z = 1$, when the preferred location of these objects is close to the universe mean ($\delta = 0$). This time-evolution pattern is independent of cosmology, as it is present both in the concordance and the Einstein-deSitter universes, and appears rather to be a characteristic of the hierarchical nature of structure formation. Parameters of this distribution can be calculated using equations (41) and (42) which, for the concordance cos-

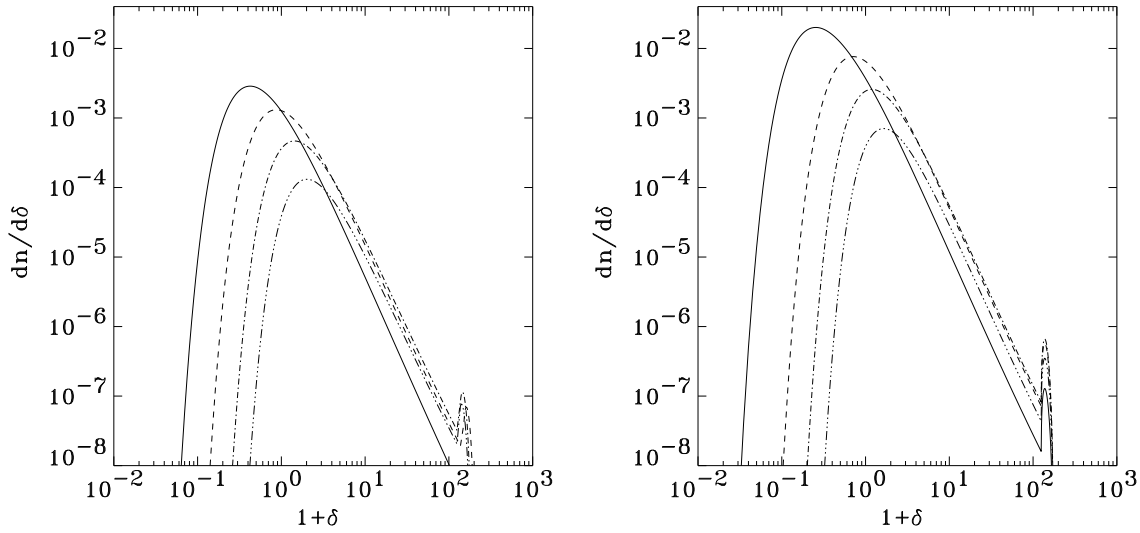

FIG. 6: Distribution of structures with respect to local density contrast, $dn/d\delta(> 10^{12}\,\mathrm{M}_\odot)$, for $\beta = 2$ and for $\Omega_\mathrm{m} + \Omega_\Lambda = 1$ (left panel) and Einstein-deSitter (right panel) universes. Solid line: $z = 0$; dashed line: $z = 1$; dot-dashed line: $z = 2$; double-dot–dashed line: $z = 3$. The units of $dn/d\delta$ are number of objects per Mpc^3.

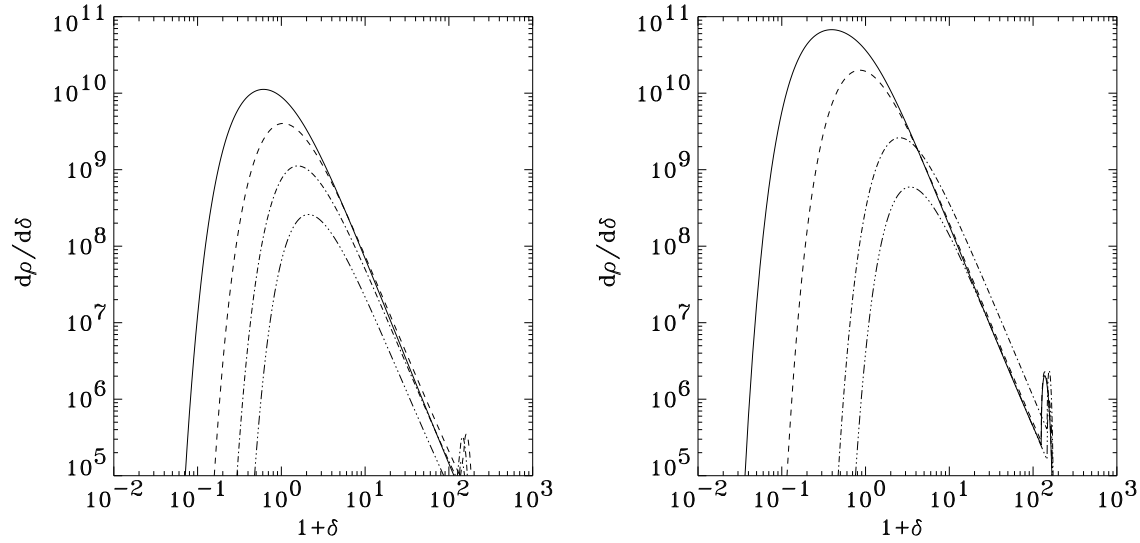

FIG. 7: Distribution of density of matter inside collapsed structures with respect to local density contrast, $d\rho/d\delta(> 10^{12}\,\mathrm{M}_\odot)$, for $\beta = 2$ and for $\Omega_\mathrm{m} + \Omega_\Lambda = 1$ (left panel) and Einstein-deSitter (right panel) universes. Solid line: $z = 0$; dashed line: $z = 1$; dot-dashed line: $z = 2$; double-dot–dashed line: $z = 3$. The units of $d\rho/d\delta$ are $\mathrm{M}_\odot$ per Mpc^3.

mology and $z = 0$ give $\langle\delta\rangle_\mathrm{n} = 0.43$ and $\sigma_{\delta,\mathrm{n}} = 4.36$. The large value of the variance shows that the distribution is significantly broad. However, the positive value of the mean is an artifact of the asymmetric boundaries of the distribution and its long high-δ tail. This is demonstrated by the notably different locations of the mean and the median. The value of the latter is $\delta = -0.22$, therefore more structures in this range reside inside underdensities.

Figure 7 is the matter-density counterpart of Figure 6, as it plots $d\rho/d\delta(> 10^{12}\mathrm{M}_\odot)$ as a function of $1 + \delta$ for the same values of redshift as in Figure 6. Again, at the current cosmic epoch, the distribution peaks at negative values of δ. Most of the virialized matter in the universe today appears to reside inside isolated objects rather than in clusters (note that decreasing the value of m_min will only enhance this result since the trend towards isolation is more pronounced for the lower-mass objects). The trend of the peak with time (towards larger δ for higher reshifts) is duplicated here as well. In particular,

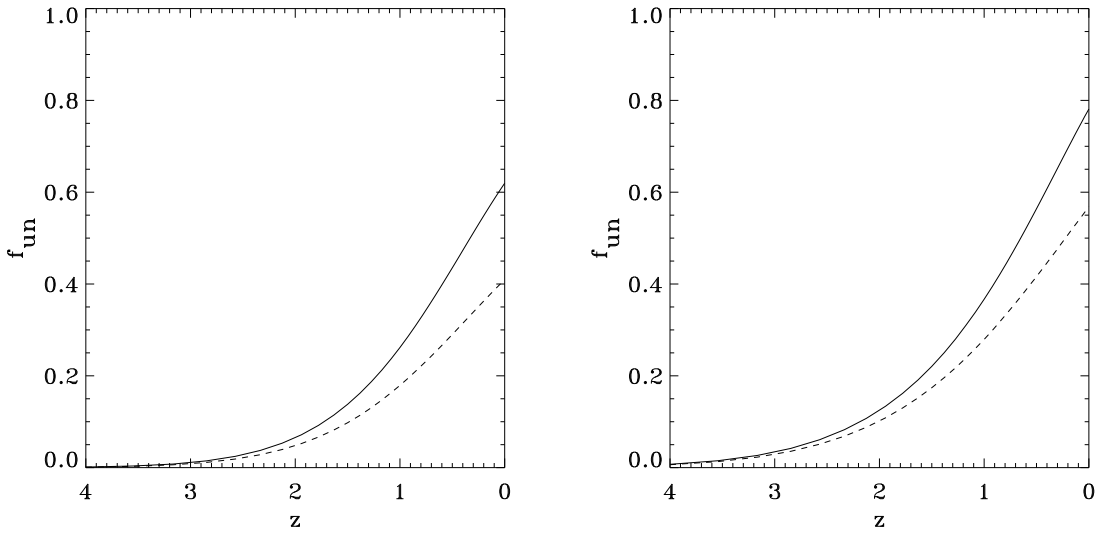

FIG. 8: Fraction by number $f_{n,\rm un}$ (solid line) and my mass $f_{\rho,\rm un}$ (dashed line) of objects of mass $> 10^{12}\,{\rm M}_\odot$ living in underdense regions, as a function of redshift, for $\Omega_{\rm m} + \Omega_\Lambda = 1$ (left panel) and Einstein-deSitter (right panel) universes.

note that at present, a significant fraction of the mass lies in moderately underdense regions. Equations (43) and (44) give for this distribution (in the concordance cosmology and for $z = 0$), $\langle\delta\rangle_\rho = 1.20$ and $\sigma_{\delta,\rho} = 6.23$. The median of this distribution is at $\delta = 0.20$, a positive value.

Finally, Figure 8 plots the evolution with redshift of the fractions by number and by mass, $f_{n,\rm un}$ and $f_{\rho,\rm un}$, of objects with $m > 10^{12}\,{\rm M}_\odot$, living inside underdense regions. At high redshifts, when the mass of such objects is well above the exponential suppression cutoff, practically none of them is found inside underdensities. This trend is reversed as the redshift decreases. In the $\Omega + \Omega_\Lambda = 1$ universe, an equal number of these structures are located inside underdensities by redshift 0.3 and by the current cosmic epoch, about 60% by number (but only 40% by mass) of these structures are located inside underdensities.

Figure 9 demonstrates the effect of changing the clustering scale parameter on the double distribution. Slices of the double distribution along $m = 5.5 \times 10^{14}\,{\rm M}_\odot$ are plotted (in linear axes) as a function of δ, and for $\beta = 1.5$ (solid line), 2 (dashed line), 3 (dot-dashed line) and 10 (double-dot–dashed line). The location of the peak appears to be extremely insensitive to the value of β for moderately low values. It very slowly moves towards $\delta = 0$ with increasing β, as it should (increasing β results in averaging the overdensity over increasingly large volumes). Note that even as β approaches 1, the peak will *not* move towards $\delta_{\rm c}$, as a result of our correction for the central-object contamination. This makes our formalism particularly suitable to study the properties of matter very close but outside a virialized structure (e.g. the local density of accreted gas).

The effect of β on an integral quantity is shown in Figure 10, which plots $dn/d\delta(> 10^{12}{\rm M}_\odot)$ for $\beta = 1.5$ (solid line), $\beta = 2$ (dashed line) and $\beta = 10$ (dot-dashed line). Again, the results are extremely insensitive to the value of β, which gives us confidence about the robustness of the location of the peak of our distributions.

IV. DISCUSSION

We have presented an extension of the Press-Schechter mass function, in the form of double distribution of structures with respect to mass and local overdensity. We have done so by introducing a clustering scale parameter $\beta > 1$, which we use to associate with each collapsed object of mass m a larger environment of mass βm. The scale parameter β can be expressed as a fucntion of the number of virial radii included in the local environment of each structure. We found that for reasonable values $\beta \sim 2$, the shape of the distribution does not depend sensitively on this parameter. Integration over linearly extrapolated overdensity returns the original Press-Schechter mass function, independently of the value of β.

We present the double distribution in terms of the true, physical, nonlinear density contrast δ. However, in calculating the distribution it is useful to identify regions using instead the overdensity obtained via linear analysis, $\tilde{\delta}$, extrapolated to the present epoch. A useful fitting function is given for the $\delta - \tilde{\delta}$ conversion.

The double distribution is useful because it allows us to have an explicit analytical if approximate description of the environment in which collapsed objects of all masses reside. Using the tools we have developed, it can be readily calculated for any flat cosmology, and evaluated

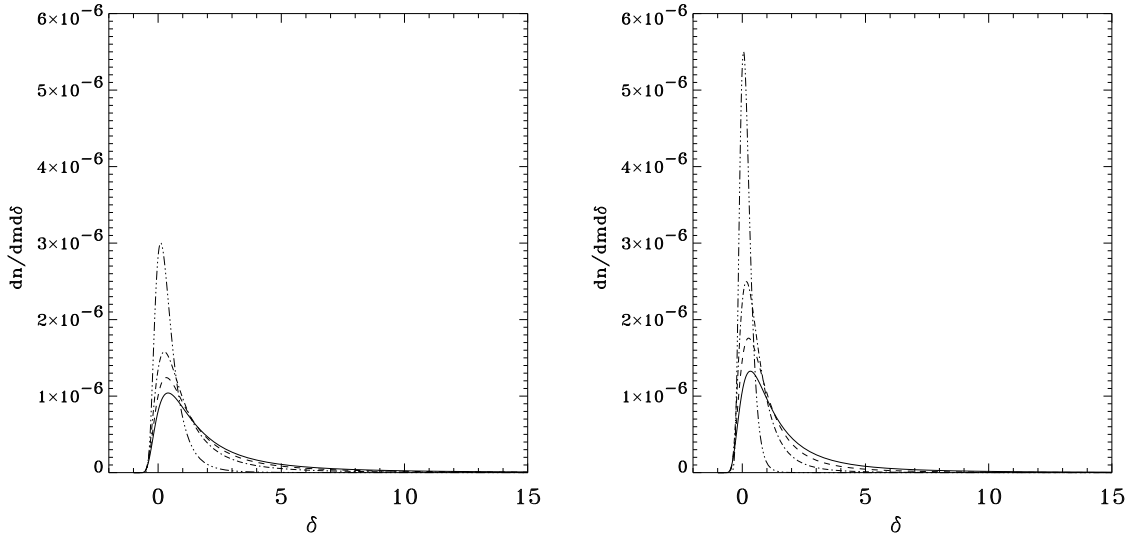

FIG. 9: Slices of the double distribution function at $m = 5.5 \times 10^{14}, \mathrm{M}_\odot$ and for different values of the clustering scale parameter β, for $\Omega_\mathrm{m} + \Omega_\Lambda = 1$ (left panel) and Einstein-deSitter (right panel) universes, plotted in linear scale. Solid line: $\beta = 1.5$; dashed line: $\beta = 2$; dot-dashed line: $\beta = 3$; double-dot–dashed line: $\beta = 10$. The units of the double distribution are number of objects per Mpc^3 per $10^{15}\mathrm{M}_\odot$.

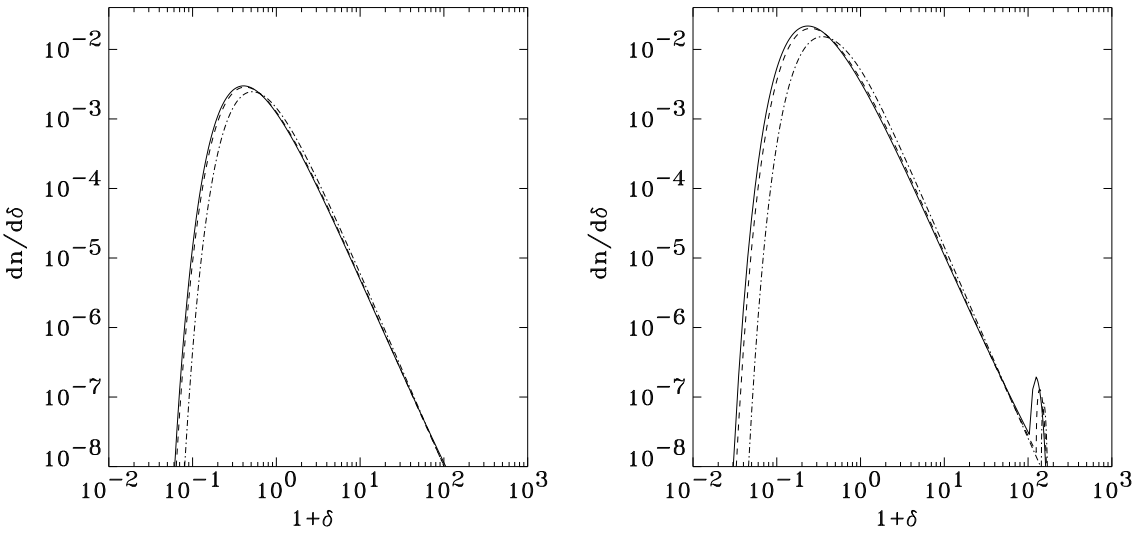

FIG. 10: Distribution of structures of mass larger than $10^{12}\,\mathrm{M}_\odot$ with respect to local density contrast, $dn/d\delta$, for $\Omega_\mathrm{m} + \Omega_\Lambda = 1$ (left panel) and Einstein-deSitter (right panel) universes, at $z = 0$, and for $\beta = 1.5$(solid line), $\beta = 2$ (dashed line) and $\beta = 10$(dot-dashed line). The units of $dn/d\delta$ are number of objects per Mpc^3.

at any epoch. Consequently, it offers new insight into the growth of structure as well as the present distribution of collapsed objects.

We have evaluated the double distribution and some of its integral moments for both a concordance cosmology and an Einstein-de Sitter universe. Some key results are that at any redshift, the double distribution is dominated by a peak which shifts in mass but is always at a relatively low value of $|\delta|$. For each mass, there is a most probable δ, which increases with structure mass. Moreover, at the present epoch in the concordance universe, the most probable environment is a modest *under*density, for all objects below about $10^{14} M_\odot$; thus, underdensities are preferentially populated by low-mass objects. Finally, the fraction of mass in underdensities increases with time, and in the concordance cosmology the present underdense mass fraction in objects of $M > 10^{12}\,\mathrm{M}_\odot$ is about 40%. These trends can be understood in terms of

hierarchical clustering in which overdense regions are the site of vigorous merging that clears out low-mass objects, which then find their last refuge in voids.

These results are consistent with other analyses in the literature which use Press-Schechter-like formalism to probe the correlations between structures. For example, [13] extend the Press-Schechter random-walk picture in a way very similar to ours, but identify a local environment in terms of a fixed, mass-independent radius. Our results are thus complementary to these, because we adopt a mass-dependent environment based on the virial radius.

Finally, it is well-known that the Press-Schechter mass function provides an excellent characterization of the results of numerical N-body simulations (e.g., [8]). It would be of great interest to compare the analytic double distribution we have presented with numerical results. We plan to address this issue in future work.

Acknowledgments

We thank Dimitris Galanakis, Telemachos Mouschovias, Kostas Tassis and Ben Wandelt for enlightening discussions. This work was supported by National Science Foundation grant AST-0092939. The work of VP was partially supported by an Amelia Earhart Fellowship.

[1] W.H. Press and P. Schechter, Astrophys. J. **187**, 425 (1974).
[2] J.R. Bond, S. Cole, G. Efstathiou, and N. Kaiser, Astrophys. J. **379**, 440 (1991).
[3] C. Lacey and S. Cole, Mon. Not. R. Astron. Soc. **262**,627 (1993)
[4] J.A. Peacock and A.F. Heavens, Mon. Not. R. Astron. Soc. **243**, 133 (1990).
[5] K. Jedamzik, Astrophys. J. **448**, 1(1995).
[6] R. Bower, Mon. Not. R. Astron. Soc. **248**, 332 (1991).
[7] S.D.M. White, G. Efstathiou, and C.S. Frenk, Mon. Not. R. Astron. Soc. **262**, 1023 (1993).
[8] C. Lacey and S. Cole, Mon. Not. R. Astron. Soc. **271**, 676 (1994).
[9] R.V. Eke, S. Cole, and C.S. Frenk, Mon. Not. R. Astron. Soc. **282**, 263 (1996).
[10] J. Lee and S.F. Shandarin, Astrophys. J. **500**, 14 (1998).
[11] R.K. Sheth, H.J. Mo, and G. Tormen, Mon. Not. R. Astron. Soc. **323**, 1 (2001).
[12] R.K. Sheth and G. Tormen, Mon. Not. R. Astron. Soc. **329**, 61 (2002).
[13] H.J. Mo and S.D.M. White, Mon. Not. R. Astron. Soc. **282**, 347 (1996).
[14] G. Kaufmann, A. Nusser & M. Steinmetz, Mon. Not. R. Astron. Soc. **286**, 795 (1997).
[15] R.K. Sheth, Mon. Not. R. Astron. Soc. **300**, 1057 (1998).
[16] M. Tegmark & P.J.E. Peebles, Astrophys. J. **500**, L79 (1998).
[17] G. Lemson & G. Kaufmann, Mon. Not. R. Astron. Soc. **302**, 111 (1999).
[18] R.K. Sheth & G. Tormen, Mon. Not. R. Astron. Soc. **308**, 119 (1999).
[19] U. Seljak, Mon. Not. R. Astron. Soc. **318**, 203 (2000).
[20] A. Cooray & R. Sheth, Phys. Rep. **372**, 1 (2002).
[21] J.P. Jing, Astrophys. J. **503**, L9 (1998).
[22] S. Chandrasekhar, Rev. Mod. Phys. **15**, 2 (1943).
[23] F. Bernardeau, Astron. & Astrophys. **291**, 697 (1994).
[24] D. N. Spergel *et al.*, Astrophys. J. Suppl. **148**, 175 (2003).
[25] J.M. Bardeen, J.R. Bond, N. Kaiser and A.S. Szalay, Astrophys. J. **304**, 15 (1986).
[26] H.J. Mo and S.D.M. White, Mon. Not. R. Astron. Soc. **336**, 112 (2002).
[27] P.J.E.Peebles, Astrophys. J. **284**, 439 (1984).
[28] G. Lemaître, Compt. Rend. **196**, 903 (1933).
[29] G. Lemaître, Compt. Rend. **196**, 1085 (1933).
[30] O. Lahav, P.B. Lilje, J.R. Primack, and M.J. Rees Mon. Not. R. Astron. Soc.**251**, 128 (1991).
[31] P.J.E. Peebles, The Large Scale Structure of the Universe, Princeton Univ. Press, Princeton, NJ (1980).
[32] The *proper* mass function, i.e. the number of collapsed structures per unit proper volume per differential mass interval is simply related to the comoving mass function via $dn/dm|_{\rm proper} = a^{-3} dn/dm|_{\rm comoving}$
[33] as seen by equation (9) re-written for the extrapolated rather than the true overdensity field
[34] Physically, the substitution of the true field by the extrapolated field in the "random walk" corresponds to smoothing the extrapolated overdensity field, and then mapping the mean extrapolated overdensity value to a true overdensity value. That true overdensity value is then assumed to accurately represent the result of a smoothing of the true field, which implies $\delta\left(\left\langle\tilde{\delta}\right\rangle\right) = \left\langle\delta\left(\tilde{\delta}\right)\right\rangle$. This would be exactly true only if $\delta(\tilde{\delta})$ was linear in $\tilde{\delta}$, which is not the case (see appendices B and C). This assumption introduces an inaccuracy inherent to all calculations which employ it, including the Press-Schechter mass function as well as the double distribution.
[35] since $S(m)$ monotonically decreases with m for all physically interesting power spectra
[36] Note however that for fixed β, the number of virial radii included in the environment depends on δ_ℓ and is larger for underdense environments.
[37] The introduction of a finite minimum mass $m_{\rm min}$ is necessary for both physical and technical reasons. Physically, the mass of collapsed objects is strictly forced to have a lower bound, not only due to the finite mass of the dark matter particle, but also due to the existence of a dark matter Jeans mass, however small this may be. Practically, the Press-Schechter dn/dm diverges as $m \to 0$ and setting a minimum mass is required to extract interesting information.

APPENDIX A: ANALYTICAL PROPERTIES OF THE DOUBLE DISTRIBUTION

1. Derivation of the Press-Schechter Mass Function From the Double Distribution

Using S_1 to denote $S(m)$ and S_2 for $S(\beta m)$ we have:

$$\begin{aligned}
\int_{-\infty}^{\tilde{\delta}_{0,c}} d\tilde{\delta}\frac{dn}{dmd\tilde{\delta}} &= \frac{\rho_m}{m}\left|\frac{dS_1}{dm}\right| \frac{1}{2\pi S_2^{1/2}(S_1-S_2)^{3/2}} \left\{ \int_{-\infty}^{\tilde{\delta}_{0,c}} d\tilde{\delta}(\tilde{\delta}_{0,c}-\tilde{\delta}) \exp\left[-\frac{\tilde{\delta}^2}{2S_2}\right] \exp\left[-\frac{(\tilde{\delta}_{0,c}-\tilde{\delta})^2}{2(S_1-S_2)}\right] - \right. \\
&\left. \int_{-\infty}^{\tilde{\delta}_{0,c}} d\tilde{\delta}(\tilde{\delta}_{0,c}-\tilde{\delta}) \exp\left[-\frac{(\tilde{\delta}-2\tilde{\delta}_{0,c})^2}{2S_2}\right] \exp\left[-\frac{(\tilde{\delta}_{0,c}-\tilde{\delta})^2}{2(S_1-S_2)}\right] \right\} \\
&= \frac{\rho_m}{m}\frac{1}{2\pi S_2^{1/2}(S_1-S_2)^{3/2}} \left|\frac{dS_1}{dm}\right| \int_{-\infty}^{\infty} \tilde{\delta}' d\tilde{\delta}' \exp\left[-\frac{(\tilde{\delta}_{0,c}-\tilde{\delta}')^2}{2S_2}\right] \exp\left[-\frac{\tilde{\delta}'^2}{2(S_1-S_2)}\right] \\
&= \frac{\rho_m}{m}\frac{1}{2\pi S_2^{1/2}(S_1-S_2)^{3/2}} \left|\frac{dS_1}{dm}\right| \tilde{\delta}_{0,c}\left(\frac{S_1-S_2}{S_1}\right)^{3/2} \sqrt{2\pi S_2} \exp\left[-\frac{\tilde{\delta}_{0,c}^2}{2S_1}\right] \\
&= \sqrt{\frac{2}{\pi}}\frac{\rho_m}{m^2}\frac{\tilde{\delta}_{0,c}}{\sqrt{S_1}}\left|\frac{d\ln\sqrt{S_1}}{d\ln m}\right| \exp\left[-\frac{\tilde{\delta}_{0,c}^2}{2S_1}\right] \qquad \text{(A1)}
\end{aligned}$$

where we performed a change of variables $\tilde{\delta}' = \tilde{\delta}_{0,c} - \tilde{\delta}$, and we set $\tilde{\delta}' \to -\tilde{\delta}'$ in the second integral. The final result is the Press-Schechter mass function formula. Note that this result is independent of the value of β.

2. Behavior of the Double Distribution in the limit $\beta \to \infty$

In order to find the behavior the double distribution as $\beta \to \infty$, we recall that, because $S(m)$ decreases monotonically with m, its limit in the infinite β regime will be

$$\lim_{\beta\to\infty} S(\beta m) = 0\,. \qquad \text{(A2)}$$

Then, using the notation of the previous section,

$$\lim_{\beta\to\infty}\frac{dn}{dmd\tilde{\delta}_\ell}(m,\tilde{\delta}_\ell,\beta,a) = \lim_{S_2\to 0}\frac{dn}{dmd\tilde{\delta}_\ell}(S_1,S_2,\tilde{\delta}_\ell,a,m)\,. \qquad \text{(A3)}$$

The limit of a unit-area Gaussian when its width vanishes is the Dirac delta-finction δ_D,

$$\lim_{\lambda\to 0}\frac{1}{\sqrt{2\pi}\lambda}\exp\left[-\frac{(x-x_0)^2}{2\lambda^2}\right] = \delta_D(x-x_0)\,. \qquad \text{(A4)}$$

Using this result, we get

$$\begin{aligned}
\lim_{S_2\to 0}\frac{dn}{dmd\tilde{\delta}_\ell} &= \frac{\rho_m}{m}\left|\frac{dS_1}{dm}\right| \frac{\tilde{\delta}_{0,c}-\tilde{\delta}_\ell}{2\pi} \lim_{S_2\to 0}\left\{ \exp\left[-\frac{(\tilde{\delta}_{0,c}-\tilde{\delta}_\ell)^2}{2(S_1-S_2)}\right] \frac{\exp\left[-\frac{\tilde{\delta}_\ell^2}{2S_2}\right] - \exp\left[-\frac{(\tilde{\delta}_\ell-2\tilde{\delta}_{0,c})^2}{2S_2}\right]}{S_2^{1/2}(S_1-S_2)^{3/2}} \right\} \\
&= \frac{\rho_m}{m}\left|\frac{dS_1}{dm}\right| \frac{\tilde{\delta}_{0,c}-\tilde{\delta}_\ell}{\sqrt{2\pi}} \frac{\exp\left[-\frac{(\tilde{\delta}_{0,c}-\tilde{\delta}_\ell)^2}{2S_1}\right]}{S_1^{3/2}} \left\{ \lim_{S_2\to 0}\frac{\exp\left[-\frac{\tilde{\delta}_\ell^2}{2S_2}\right]}{\sqrt{2\pi S_2}} - \lim_{S_2\to 0}\frac{\exp\left[-\frac{(\tilde{\delta}_\ell-2\tilde{\delta}_{0,c})^2}{2S_2}\right]}{\sqrt{2\pi S_2}} \right\} \\
&= \frac{\rho_m}{m}\left|\frac{dS_1}{dm}\right| \frac{\tilde{\delta}_{0,c}-\tilde{\delta}_\ell}{\sqrt{2\pi}} \frac{\exp\left[-\frac{(\tilde{\delta}_{0,c}-\tilde{\delta}_\ell)^2}{2S_1}\right]}{S_1^{3/2}} \left[\delta_D(\tilde{\delta}_\ell) - \delta_D(\tilde{\delta}_\ell - 2\tilde{\delta}_{0,c})\right]\,. \qquad \text{(A5)}
\end{aligned}$$

However, the $\tilde{\delta}_\ell-$domain of the double distribution is between $-\infty$ and $\tilde{\delta}_{0,\rm c}$, and therefore the value $\tilde{\delta}_\ell = 2\tilde{\delta}_{0,\rm c}$ is outside its domain. Hence the second Dirac delta-function is always zero, and

$$\lim_{\beta\to\infty}\frac{dn}{dmd\tilde{\delta}_\ell} = \frac{\rho_{\rm m}}{m}\left|\frac{dS_1}{dm}\right|\frac{\tilde{\delta}_{0,\rm c}-\tilde{\delta}_\ell}{\sqrt{2\pi}}\frac{\exp\left[-\frac{(\tilde{\delta}_{0,\rm c}-\tilde{\delta}_\ell)^2}{2S_1}\right]}{S_1^{3/2}}\delta_{\rm D}(\tilde{\delta}_\ell)\,, \tag{A6}$$

proportional, as expected, to a Dirac delta-function centered at $\tilde{\delta}_\ell = 0$.

3. Behavior of the Double Distribution in the limit $\beta \to 1$

Denoting $S(\beta m)$ by S_2 and letting $\phi = S(m)/S(\beta m)$, we seek the behavior of the double distribution in the limit $\beta \to 1$ or $\phi \to 1$. Defining

$$\mathcal{C} = \frac{\rho_{\rm m}}{m}\frac{\tilde{\delta}_{0,\rm c}-\tilde{\delta}_\ell}{\sqrt{2\pi}}\left|\frac{dS}{dm}\right|\frac{\exp\left[-\frac{\tilde{\delta}_\ell^2}{2S_2}\right]-\exp\left[-\frac{(\tilde{\delta}_\ell-2\tilde{\delta}_{0,\rm c})^2}{2S_2}\right]}{S_2^{1/2}}\,, \tag{A7}$$

we can write

$$\begin{aligned}
\lim_{\phi\to1}\frac{dn}{dmd\tilde{\delta}_\ell} &= \mathcal{C}\lim_{\phi\to1}\frac{\exp\left[-\frac{(\tilde{\delta}_{0,\rm c}-\tilde{\delta}_\ell)^2}{2S_2(\phi-1)}\right]}{\sqrt{2\pi}S_2^{3/2}(\phi-1)^{3/2}}\\
&= \mathcal{C}\lim_{\phi\to1}\frac{(\phi-1)^{-3/2}}{\sqrt{2\pi}S_2^{3/2}\exp\left[\frac{(\tilde{\delta}_{0,\rm c}-\tilde{\delta}_\ell)^2}{2S_2(\phi-1)}\right]}\\
&\overset{\infty/\infty}{=} \mathcal{C}\lim_{\phi\to1}\frac{-\frac{3}{2}(\phi-1)^{-5/2}}{\exp\left[\frac{(\tilde{\delta}_{0,\rm c}-\tilde{\delta}_\ell)^2}{2S_2(\phi-1)}\right]\left[-\frac{\sqrt{2\pi}S_2^{3/2}(\tilde{\delta}_{0,\rm c}-\tilde{\delta}_\ell)^2}{2S_2(\phi-1)^2}\right]}\\
&= \mathcal{C}\lim_{\phi\to1}\frac{3\exp\left[-\frac{(\tilde{\delta}_{0,\rm c}-\tilde{\delta}_\ell)^2}{2S_2(\phi-1)}\right]}{\sqrt{2\pi}S_2^{1/2}(\phi-1)^{1/2}(\tilde{\delta}_{0,\rm c}-\tilde{\delta}_\ell)^2}\\
&= \mathcal{C}\frac{3}{(\tilde{\delta}_{0,\rm c}-\tilde{\delta}_\ell)^2}\delta_{\rm D}(\tilde{\delta}_{0,\rm c}-\tilde{\delta}_\ell)
\end{aligned} \tag{A8}$$

proportional, as expected, to a Dirac delta-function around $\tilde{\delta}_{0,\rm c}$.

APPENDIX B: RELATING LINEARLY EXTRAPOLATED AND TRUE OVERDENSITIES IN AN EINSTEIN-DE SITTER ($\Omega_{\rm M} = 1$) COSMOLOGY

In this appendix we derive a conversion relation $\tilde{\delta}_0(a,\delta)$ for an $\Omega_{\rm m} = 1$ cosmology (here, δ is the density contrast predicted for a density perturbation at cosmic epoch a by the spherical evolution model and $\tilde{\delta}_0$ is the extrapolation of the density contrast to the present cosmic epoch using linear theory). In order to do so, we first calculate $\delta(a)$ from the spherical evolution solution, then calculate $\tilde{\delta}_0$ using linear theory, and finally require that $\delta(a)$ and $\tilde{\delta}_a$ (the linear-theory density contrast at epoch a) should agree at early times.

1. Spherical Evolution Model in an $\Omega_{\rm m} = 1$ Universe

The evolution of a spherically symmetric, overdense perturbation in an otherwise homogeneous $\Omega_{\rm m} = 1$ universe is described by the parametric equations

$$a_{\rm p} = \frac{2a_{\rm coll}}{(12\pi)^{2/3}}(1-\cos\theta)\,,\ \text{and}\ a = a_{\rm coll}\left(\frac{\theta-\sin\theta}{2\pi}\right)^{2/3}\,, \tag{B1}$$

where $a_{\rm coll}$ is the scale factor of the universe when the perturbation formally collapses to a point, $a_{\rm p}$ is the scale factor of the perturbation, and θ is the development angle. Note that the perturbation will turn around (reach its maximum size, $a_{\rm p,max} = 4a_{\rm coll}(12\pi)^{-2/3}$) when $\theta = \pi$, at a time $a = a_{\rm coll}/2^{2/3}$.

The normalization of equation B1 is such that the density contrast δ can be expressed as

$$\delta = \left(\frac{a}{a_{\rm p}}\right)^3 - 1\,. \tag{B2}$$

Hence, for any density contrast δ, equations B1 and B2 can be combined to give a unique development angle $\theta(\delta)$ which is the solution to the transcendental equation

$$\frac{6^{2/3}(\theta-\sin\theta)^{2/3}}{2(1-\cos\theta)} - (1+\delta)^{1/3} = 0\,. \tag{B3}$$

Similarly, the spherical evolution solution for an underdensity is given by the parametric equations

$$a_{\rm p} = A_{\rm p}(\cosh\eta - 1)\,,\ \text{and}\ a = A_{\rm p}\frac{6^{2/3}}{2}(\sinh\eta-\eta)^{2/3}\,. \tag{B4}$$

where η is the development angle in this case. Equation B4 together with equation B2 can be combined as before to give $\eta(\delta)$ as the solution to the transcendental equation

$$\frac{6^{2/3}(\sinh\eta-\eta)^{2/3}}{2(\cosh\eta-1)} - (1+\delta)^{1/3} = 0\,. \tag{B5}$$

2. $\tilde{\delta}_0(a,\delta)$ according to the spherical evolution model

The behavior of δ in the linear regime in this cosmology is

$$\tilde{\delta} = \tilde{\delta}_0 a\,. \tag{B6}$$

This result should coincide with the linear expansion of the spherical evolution result at early times. Expanding

the parametric solution to second nonvanishing order in θ and eliminate θ, we obtain

$$a_{\rm p}(a) = a\left[1 - \frac{(12\pi)^{2/3}}{20}\frac{a}{a_{\rm coll}}\right]. \tag{B7}$$

We then substitute equation B7 in the definition of δ (eq. B2) to get

$$\tilde{\delta} = \frac{3(12\pi)^{2/3}}{20 a_{\rm coll}} a \tag{B8}$$

which, by comparison to equation B6 gives

$$\tilde{\delta}_0 = \frac{3(12\pi)^{2/3}}{20 a_{\rm coll}}. \tag{B9}$$

Then, the conversion relation we seek is

$$\tilde{\delta}_0(a,\delta) = \frac{6^{2/3}3}{20a}\left[\theta(\delta) - \sin\theta(\delta)\right]^{2/3} \tag{B10}$$

where $\theta(\delta)$ is given by equation B3.

Equation B10 has the undesirable property that it diverges as θ approaches 2π. This is of course a consequence of the perturbation formally collapsing to a singularity in the spherical evolution model instead of reaching virial equilibrium. If we make the usual assumption that at virialization the radius of the perturbation is $a_{\rm max}/2$ and we additionally require that

- $\tilde{\delta}_0(a,\delta)$ is continuous and smooth at $\theta = 3\pi/2$
- $a_{\rm p} = a_{\rm p,max}$ for all $a \geq a_{\rm coll}$

then for $\theta > 3\pi/2$ (which corresponds to $\delta > 9(3\pi+2)^2/8$) we can replace equation B10 with

$$\begin{aligned}\tilde{\delta}_0(a,\delta) &= \tilde{\delta}_{0,\rm v} + \tilde{\delta}'_{0,\rm v}(\delta - \delta_{\rm v}) \\ &+ \frac{3(\tilde{\delta}_{0,\rm c} - \tilde{\delta}_{0,\rm v}) - (\delta_{\rm c} - \delta_{\rm v})(2\tilde{\delta}'_{0,\rm v} + \tilde{\delta}'_{0,c})}{(\delta_{\rm c} - \delta_{\rm v})^2}(\delta - \delta_{\rm v})^2 \\ &+ \frac{(\tilde{\delta}'_{0,\rm c} + \tilde{\delta}'_{0,\rm v})(\delta_{\rm c} - \delta_{\rm v}) - 2(\tilde{\delta}_{0,\rm c} - \tilde{\delta}_{0,\rm v})}{(\delta_{\rm c} - \delta_{\rm v})^3}(\delta - \delta_{\rm v})^3\end{aligned} \tag{B11}$$

(see appendix C for a discussion of the reasons for employing this particular functional form, and §II and III for a discussion on why the effect of such a choice on the double distribution is negligible). In equation B11,

$$\begin{aligned}\delta_{\rm v} &= \left(\frac{a|_{\theta=3\pi/2}}{a_{\rm p}|_{\theta=3\pi/2}}\right)^3 - 1 = \frac{9(3\pi+2)^2}{8} - 1 \\ \delta_{\rm c} &= \left(\frac{a|_{\theta=2\pi}}{a_{\rm p}|_{\theta=3\pi/2}}\right)^3 - 1 = 18\pi^2 - 1 \\ \tilde{\delta}_{0,\rm v} &= \tilde{\delta}_0(a,\delta_{\rm v}) = \frac{3^{5/3}}{20a}(3\pi+2)^{2/3} \\ \tilde{\delta}'_{0,\rm c} &= \left.\frac{\partial\tilde{\delta}_0}{\partial\delta}\right|_{\delta=\delta_{\rm c}} = \frac{1}{10a(1+\delta_{\rm c})^{2/3}}\end{aligned} \tag{B12}$$

The last equality coming from the fact that after $a_{\rm coll}$ the radius of a perturbation remains constant and equal to $a_{\rm p,max}/2$, while its density contrast δ changes only due to the expansion of the background universe, $\delta = (2a/a_{\rm p,max})^3 - 1$ or $\delta = (10a\tilde{\delta}_0/3)^3 - 1$. Finally, $\tilde{\delta}_{0,\rm c}$ is given by equation B17 while $\tilde{\delta}'_{0,\rm v}$ is given by equation B18 for $\delta = \delta_{\rm v}$ and $\theta = 3\pi/2$.

To get the linear behavior of δ for an underdensity we expand the parametric solution B4 to second nonvanishing order in η and we eliminate η to get

$$a_{\rm p} = A_{\rm p}\frac{6^{2/3}}{2}\left[1 + \frac{1}{10}\frac{a}{A_{\rm p}}\right]. \tag{B13}$$

Substituting equation B13 in the definition of δ (eq. B2), we get for the time dependence of δ at early times,

$$\tilde{\delta} = -\frac{3}{10A_{\rm p}}a \tag{B14}$$

from which, by comparison to equation B6, we get

$$\tilde{\delta}_0 = -\frac{3}{10A_{\rm p}}. \tag{B15}$$

Then, $\tilde{\delta}_0(a,\delta)$ will be

$$\tilde{\delta}_0(a,\delta) = -\frac{6^{2/3}3}{20a}\left[\sinh\eta(\delta) - \eta(\delta)\right]^{2/3} \tag{B16}$$

where $\eta(\delta)$ is given by equation B5.

Equation B16 is valid for all η and its limit as $\tilde{\delta} \to -\infty$ is $\delta(\tilde{\delta}) \to -1$. Thus, although the linearly extrapolated field can become < -1, the corresponding value of the actual δ is always ≥ -1, as the physical requirement $\rho_{\rm p} \geq 0$ demands.

3. Critical extrapolated overdensity for collapse, $\tilde{\delta}_{0,\rm c}(a)$

The critical extrapolated overdensity for collapse can be found from equation B9

$$\tilde{\delta}_{0,\rm c}(a_{\rm coll}) = \frac{3(12\pi)^{2/3}}{20}a_{\rm coll}^{-1} \approx 1.69 a_{\rm coll}^{-1}. \tag{B17}$$

Note that the above equation has the functional form $\tilde{\delta}_{0,\rm c}(a_{\rm coll}) \propto 1/D(a_{\rm coll})$, where $D(a)$ is the linear growth factor for this cosmology. This is also true in the $\Omega_{\rm m} + \Omega_\Lambda = 1$ case.

4. $\partial\tilde{\delta}_0/\partial\delta|_a$

In addition to the relation between δ and $\tilde{\delta}_0$, we will also need the derivative $\partial\tilde{\delta}_0/\partial\delta|_a$ in order to convert between true and extrapolated overdensity differentials in

equation (16). In the case of an overdense structure, $\delta > 0$, equation B10 gives

$$\left.\frac{\partial\tilde{\delta}_0}{\partial\delta}\right|_a = \frac{6^{2/3}}{10a}\frac{1-\cos\theta(\delta)}{[\theta(\delta)-\sin\theta(\delta)]^{1/3}}\frac{d\theta}{d\delta}\,. \tag{B18}$$

To evaluate $d\theta/d\delta$ we define the auxiliary function

$$F_{\rm a}(\theta,\delta) = 6^{2/3}(\theta-\sin\theta)^{2/3} - 2(1-\cos\theta)(1+\delta)^{1/3}\,. \tag{B19}$$

From equation B3 we get immediately $F_{\rm a}(\theta,\delta)=0$, and differentiating we get $dF_{\rm a} = 0 = \frac{\partial F_{\rm a}}{\partial\theta}d\theta + \frac{\partial F_{\rm a}}{\partial\delta}d\delta$. Hence,

$$\frac{d\theta}{d\delta} = -\frac{\partial F_{\rm a}}{\partial\delta}\left(\frac{\partial F_{\rm a}}{\partial\theta}\right)^{-1}\,, \tag{B20}$$

where

$$\frac{\partial F_{\rm a}}{\partial\delta} = -\frac{2}{3}\frac{1-\cos\theta}{(1+\delta)^{2/3}} \tag{B21}$$

and

$$\frac{\partial F_{\rm a}}{\partial\theta} = \frac{6^{2/3}2}{3}\frac{1-\cos\theta}{(\theta-\sin\theta)^{1/3}} - 2(1+\delta)^{1/3}\sin\theta\,. \tag{B22}$$

Equation B18 is valid only for $0<\delta<\delta_{\rm v}$. For $\delta>\delta_{\rm v}$ equation B11 gives

$$\begin{aligned}\left.\frac{\partial\tilde{\delta}_0}{\partial\delta}\right|_a \;=\; & \tilde{\delta}'_{0,{\rm v}} \\ & +2\frac{3(\tilde{\delta}_{0,{\rm c}}-\tilde{\delta}_{0,{\rm v}})-(\delta_{\rm c}-\delta_{\rm v})(2\tilde{\delta}'_{0,{\rm v}}+\tilde{\delta}'_{0,c})}{(\delta_{\rm c}-\delta_{\rm v})^2}(\delta-\delta_{\rm v}) \\ & +3\frac{(\tilde{\delta}'_{0,{\rm c}}+\tilde{\delta}'_{0,{\rm v}})(\delta_{\rm c}-\delta_{\rm v})-2(\tilde{\delta}_{0,{\rm c}}-\tilde{\delta}_{0,{\rm v}})}{(\delta_{\rm c}-\delta_{\rm v})^3}(\delta-\delta_{\rm v})^2\,.\end{aligned} \tag{B23}$$

In the case of an underdense structure, $\delta<0$, equation B16 gives

$$\left.\frac{\partial\tilde{\delta}_0}{\partial\delta}\right|_a = -\frac{6^{2/3}}{10a}\frac{\cosh\eta(\delta)-1}{[\sinh\eta(\delta)-\eta(\delta)]^{1/3}}\frac{d\eta}{d\delta}\,. \tag{B24}$$

As before, in order to evaluate $d\eta/d\delta$ we define the auxiliary function

$$G_{\rm a}(\eta,\delta) = 6^{2/3}(\sinh\eta-\eta)^{2/3} - 2(\cosh\eta-1)(1+\delta)^{1/3}\,. \tag{B25}$$

Equation B5 implies $G_{\rm a}(\eta,\delta)=0$ so

$$\frac{d\eta}{d\delta} = -\frac{\partial G_{\rm a}}{\partial\delta}\left(\frac{\partial G_{\rm a}}{\partial\eta}\right)^{-1}\,, \tag{B26}$$

where

$$\frac{\partial G_{\rm a}}{\partial\delta} = -\frac{2}{3}\frac{\cosh\eta-1}{(1+\delta)^{2/3}}\,, \tag{B27}$$

and

$$\frac{\partial G_{\rm a}}{\partial\eta} = \frac{6^{2/3}2}{3}\frac{\cosh\eta-1}{(\sinh\eta-\eta)^{1/3}} - 2(1+\delta)^{1/3}\sinh\eta\,. \tag{B28}$$

APPENDIX C: RELATING LINEARLY EXTRAPOLATED AND TRUE OVERDENSITIES IN AN $\Omega_{\rm M}+\Omega_\Lambda=1$ COSMOLOGY

In this appendix we will derive a conversion between true and extrapolated overdensity, $\delta(\tilde{\delta}_0,a)$ for an $\Omega_{\rm m}+\Omega_\Lambda=1$ cosmological model. We will do so by first calculating the true density contrast $\delta(a)$ of a density perturbation at cosmic epoch a as predicted by the spherical evolution model, then calculating $\tilde{\delta}_0$, which is the overdensity of the same spherical perturbation if extrapolated according to the linear theory until the present cosmic epoch, and finally requiring that at early times linear theory and the linear expansion of the spherical evolution model should give the same result.

1. Spherical Evolution Model in an $\Omega_{\rm m}+\Omega_\Lambda=1$ Cosmology

a. *The Evolution Equation*

In the spherical evolution model, the spherical density perturbation under consideration behaves as an independent non-flat sub-universe. Its evolution is dictated by a Friedmann equation,

$$\left(\frac{da_{\rm p}}{dt}\right)^2 = H_0^2\Omega_{\rm m}a_{\rm p}^2\left(a_{\rm p}^{-3}+\omega-\kappa a_{\rm p}^{-2}\right) \tag{C1}$$

where $a_{\rm p}$ is the radius of such a spherical density perturbation in an otherwise homogeneous universe, $\omega = \Omega_\Lambda/\Omega_{\rm m} = \Omega_{\rm m}^{-1}-1$ (where $\Omega_{\rm m}$ and Ω_Λ are the matter and vacuum density parameters of the background universe) and κ is a constant characteristic of the amplitude and sign of the perturbation: the larger the $|\kappa|$, the larger the deviation from homogeneity at a given time, while a positive κ corresponds to an overdensity and a negative κ to an underdensity. Clearly then in equation C1, the first term in parentheses on the RHS is the matter term, the second is the vacuum term and the third is the curvature term, which can have a positive or negative sign depending on whether we are studying an "open" (underdensity) or "closed" (overdensity) perturbation. The normalization of $a_{\rm p}$ is such that, had the specific spherical region begun its evolution with no curvature ($\kappa=0$), $a_{\rm p}$ at the present cosmic epoch would have been $a_{p(\kappa=0),0}=1$. For this reason, the density contrast δ of the perturbation at epoch a is given by equation B2

The behavior of the perturbation radius a_p as a function of the universe scale factor a can be found by taking the ratio of the Friedmann equations of the perturbation and the background universe, thus obtaining [27]

$$\left(\frac{da_{\rm p}}{da}\right)^2 = \frac{a_{\rm p}^{-1}+\omega a_{\rm p}^2-\kappa}{a^{-1}+\omega a^2} = \frac{a}{a_{\rm p}}\frac{\omega a_{\rm p}^2-\kappa a_{\rm p}+1}{\omega a^3+1}\,. \tag{C2}$$

Equation C2 implies that the smallest positive perturbation which will turn around and collapse corresponds to

the smallest positive κ for which the equation

$$\omega a_{\rm p}^3 - \kappa a_{\rm p} + 1 = 0 \tag{C3}$$

has a real positive solution [9]. This gives

$$\kappa_{\rm min,coll} = 3\omega^{1/3}/2^{2/3}\,. \tag{C4}$$

Equation C2 can then be re-written as

$$\frac{da_{\rm p}}{da} = \begin{cases} \left(\frac{a_{\rm p}^{-1}+\omega a_{\rm p}^2-\kappa}{a^{-1}+\omega a^2}\right)^{1/2}, & \kappa < \kappa_{\rm min,coll} \quad \textbf{or} \\ & \kappa \geq \kappa_{\rm min,coll},\ a < a_{\rm ta} \\ -\left(\frac{a_{\rm p}^{-1}+\omega a_{\rm p}^2-\kappa}{a^{-1}+\omega a^2}\right)^{1/2}, & \kappa \geq \kappa_{\rm min,coll},\ a > a_{\rm ta} \end{cases} \tag{C5}$$

where $a_{\rm ta}$ is the scale factor of the universe when the perturbation reaches its maximum (or *turnaround*) radius. The turnaround radius is the smallest of the two positive solutions of equation C3,

$$a_{\rm p,ta} = \omega^{-1/3}\sqrt{\frac{4}{3}\frac{\kappa}{\omega^{\frac{1}{3}}}}\cos\frac{1}{3}\left(\cos^{-1}\sqrt{\frac{27}{4}\left(\frac{\kappa}{\omega^{\frac{1}{3}}}\right)^{-3}}+\pi\right). \tag{C6}$$

Equation C6 has an asymptotic behavior $a_{\rm p,ta} \approx 1/\kappa$ when $\kappa/\omega^{1/3} \gg 1$, as expected from equation C3. The maximum possible turnaround radius, $a_{\rm p,ta,max}$ is achieved for $\kappa = \kappa_{\rm min,coll}$ and is $a_{\rm p,ta,max} = (2\omega)^{-1/3}$. All other collapsing overdensities will have $a_{\rm p,ta} < a_{\rm p,ta,max}$.

b. Qualitative Description of the Evolution of Structures

The introduction of the additional vacuum term in the Friedmann equation considerably complicates the simple classification of density perturbations to overdensities (all of which turn around and collapse in an $\Omega_{\rm m} = 1$ cosmology) and underdensities (all of which expand forever). In the $\Omega_{\rm m} + \Omega_\Lambda = 1$ universe there exist overdensities which will continue to expand forever. The behavior of a perturbation in such a cosmology is parametrized by the quantity $\kappa/\omega^{1/3}$, and we can identify the following cases.

Case I, $\kappa/\omega^{1/3} \leq -1$: large underdensities, expanding forever. The table below shows the relative magnitude of the three terms in the Friedmann equation (matter, curvature and vacuum term) for different values of the scale factor of the perturbation. The first line in the table indicates the hierarchy of the three terms, from largest to smaller, for each range of the scale factor. The second line indicates the dominant term in each scale factor range. The third line shows the approximate dependence of the radius of the perturbation, $a_{\rm p}$, on time, assuming that only the dominant term contributes to the Friedmann equation in each range.

$a_{\rm p} < \frac{1}{\lvert\kappa\rvert}$	$\frac{1}{\lvert\kappa\rvert} < a_{\rm p} < \frac{1}{\sqrt[3]{\omega}}$	$\frac{1}{\sqrt[3]{\omega}} < a_{\rm p} < \sqrt{\frac{\lvert\kappa\rvert}{\omega}}$	$a_{\rm p} > \sqrt{\frac{\lvert\kappa\rvert}{\omega}}$
MCV	CMV	CVM	VCM
matter	curvature	curvature	vacuum
$a_{\rm p} \sim t^{2/3}$	$a_{\rm p} \sim t$	$a_{\rm p} \sim t$	$a_{\rm p} \sim {\rm e}^t$

Case II, $-1 < \kappa/\omega^{1/3} \leq 1$: small perturbations, expanding forever. These can be either underdensities ($\kappa < 0$) or overdensities ($\kappa > 0$). In both cases the curvature term never becomes dominant. The following table shows their different evolutionary stages (as in Case I).

$a_{\rm p} < \sqrt{\frac{\lvert\kappa\rvert}{\omega}}$	$\sqrt{\frac{\lvert\kappa\rvert}{\omega}} < a_{\rm p} < \frac{1}{\sqrt[3]{\omega}}$	$\frac{1}{\sqrt[3]{\omega}} < a_{\rm p} < \frac{1}{\lvert\kappa\rvert}$	$a_{\rm p} > \frac{1}{\lvert\kappa\rvert}$
MCV	MVC	VMC	VCM
matter	matter	vacuum	vacuum
$a_{\rm p} \sim t^{2/3}$	$a_{\rm p} \sim t^{2/3}$	$a_{\rm p} \sim {\rm e}^t$	$a_{\rm p} \sim {\rm e}^t$

Case III, $1 < \kappa/\omega^{1/3} < 3/2^{2/3}$: "coasting" overdensities, expanding forever. These overdensities continue to expand forever despite the fact that they go through a phase in their evolution when the curvature term becomes dominant and their expansion slows down. During this phase, the contributions of the matter and vacuum terms, which are the ones driving the expansion, add up to a value always higher than the curvature term, although the curvature term is larger than each one of them. When the perturbation enters the curvature-dominated phase, the expansion rate decreases and the perturbation grows much more mildly than $t^{2/3}$. The expansion rate reaches a minimum at $a_{\rm p} = (2\omega)^{-1/3}$, after which it increases again as the perturbation approaches the phase of exponential expansion. This phase between the matter-like expansion and the exponential expansion is denoted by $(*)$ in the table below.

$a_{\rm p} < \frac{1}{\kappa}$	$\frac{1}{\kappa} < a_{\rm p} < \frac{1}{\sqrt[3]{\omega}}$	$\frac{1}{\sqrt[3]{\omega}} < a_{\rm p} < \sqrt{\frac{\kappa}{\omega}}$	$a_{\rm p} > \sqrt{\frac{\kappa}{\omega}}$
MCV	CMV	CVM	VCM
matter	curvature	curvature	vacuum
$a_{\rm p} \sim t^{2/3}$	$(*)$	$(*)$	$a_{\rm p} \sim {\rm e}^t$

Cases I-III are all sub-cases of the Lemaître model ([28], [29]), which features an inflection point at $a_{\rm p,e} = (2\omega)^{-1/3}$ where $\ddot{a}_{\rm p} = 0$ while $\dot{a}_{\rm p} > 0$. The rate of expansion initially decreases to achieve its minimum (positive) value when $a_{\rm p} = a_{\rm p,e}$, after which point the expansion accelerates again.

Special Case, $\kappa/\omega^{1/3} = 3/2^{2/3}$: Eddington Overdensity. This overdensity is the lowest κ overdensity which does not expand to an infinite radius. However, it does not turn around and collapse, but it approaches its (finite) turnaround radius, $a_{\rm p,max} = (2\omega)^{-1/3}$ (from eq. C6) as $t \to \infty$. As seen by an observer inside this overdensity, as $t \to \infty$ the part of the universe outside $a_{\rm p,max}$ will accelerate away and eventually exit the horizon, and the observable universe ("local Eddington bubble") will asymptotically approach the Einstein

TABLE I: Characteristic times of the spherical evolution model in an $\Omega_{\rm m}+\Omega_\Lambda=1$ universe.

event	**time**
turnaround	$t_{\rm ta}=\frac{1}{H_0\sqrt{\Omega_{\rm m}}}\int_0^{a_{\rm p,ta}} da_{\rm p}\sqrt{\frac{a_{\rm p}}{\omega a_{\rm p}^3-\kappa a_{\rm p}+1}}$
matter-vacuum equality	$t_{\rm MV}=\frac{1}{H_0\sqrt{\Omega_{\rm m}}}\int_0^{\omega^{-1/3}} da_{\rm p}\sqrt{\frac{a_{\rm p}}{\omega a_{\rm p}^3-\kappa a_{\rm p}+1}}$
matter-curvature equality	$t_{\rm MC}=\frac{1}{H_0\sqrt{\Omega_{\rm m}}}\int_0^{\lvert\kappa\rvert^{-1}} da_{\rm p}\sqrt{\frac{a_{\rm p}}{\omega a_{\rm p}^3-\kappa a_{\rm p}+1}}$
curvature-vacuum equality	$t_{\rm CV}=\frac{1}{H_0\sqrt{\Omega_{\rm m}}}\int_0^{\sqrt{\frac{\lvert\kappa\rvert}{\omega}}} da_{\rm p}\sqrt{\frac{a_{\rm p}}{\omega a_{\rm p}^3-\kappa a_{\rm p}+1}}$

static universe (as in the Eddington model with a cosmological constant).

Case IV, $\kappa/\omega^{1/3}>3/2^{2/3}$: large overdensities, eventually collapsing. When such a structure enters the dominant-curvature-term phase, its expansion rate starts to decrease ($a_{\rm p}\sim t^\epsilon$ with $\epsilon=\epsilon(t)$ monotonically decreasing from 2/3 to 0), until the expansion halts, at $a_{\rm p}=a_{\rm p,ta}$ which occurs at a time $t_{\rm ta}$, given in table I. After $t_{\rm ta}$ the perturbation turns around and contracts, its evolution being symmetrical in time about $t_{\rm ta}$, i.e. $a_{\rm p}(t)=a_{\rm p}(2t_{\rm ta}-t)$ for $t>t_{\rm ta}$ (this is a consequence of eq. C1 and holds for any cosmological model as long as the RHS of the Friedmann equation involves no explicit time-dependence). Eventually, the perturbation will formally collapse to a singularity at time $t_{\rm coll}=2t_{\rm ta}$.

$a_{\rm p}<\frac{1}{\kappa}$	$\frac{1}{\kappa}<a_{\rm p}<a_{\rm p,ta}$	$a_{\rm p,ta}>a_{\rm p}>\frac{1}{\kappa}$	$\frac{1}{\kappa}>a_{\rm p}$
MCV	CMV	CMV	MCV
matter	curvature	curvature	matter
$a_{\rm p}\sim t^{2/3}$	$a_{\rm p}\sim t^\epsilon$	$a_{\rm p}\sim(2t_{\rm ta}-t)^\epsilon$	$a_{\rm p}\sim(2t_{\rm ta}-t)^{2/3}$
expansion	expansion	contraction	contraction

In all of the cases discussed above, the transitions between different phases of their evolution occur at characteristic times, those of matter-vacuum equality $t_{\rm MV}$, matter-curvature equality $t_{\rm MC}$ and curvature-vacuum equality $t_{\rm CV}$. At these times (shown in table I), the corresponding terms in the Friedmann equation become equally important. Note that in the case of the Eddington overdensity and of case IV collapsing overdensities, matter-vacuum equality and curvature-vacuum equality are never reached, and the vacuum term never dominates over any of the other terms.

In the next section we derive exact solutions for the time-evolution of $a_{\rm p}$ for perturbations of different curvature. However, surprisingly accurate approximate solutions can be derived using only linear theory and equation (26). Solving for the spherical collapse density contrast we get

$$\delta_a\approx\left(1-\frac{\tilde\delta_a}{\tilde\delta_{\rm c}}\right)^{-\tilde\delta_{\rm c}}-1\,. \tag{C7}$$

Since $a_{\rm p}=a(1+\delta_a)^{-1/3}$, we can write for collapsing overdensities

$$\begin{aligned} a_{\rm p} &\approx a\left[1-\frac{\tilde\delta_{\rm c}D(a)/D(a_{\rm c})}{\tilde\delta_{\rm c}}\right]^{\tilde\delta_{\rm c}/3} \\ &= a\left[1-\frac{D(a)}{D(a_{\rm coll})}\right]^{\tilde\delta_{\rm c}/3}\,. \end{aligned} \tag{C8}$$

where the initial conditions (curvature) of the perturbation are parametrized by its collapse epoch, $a_{\rm coll}$, while the cosmology enters through the functional form of the linear growth factor and the linear collapse overdensity, $\tilde\delta_{\rm c}$. Similarly, for perturbations which expand for ever we can write

$$\begin{aligned} a_{\rm p} &\approx a\left[1-\frac{\tilde\delta_0 D(a)/D(a_0)}{\tilde\delta_{\rm c}}\right]^{\tilde\delta_{\rm c}/3} \\ &= a\left[1-\frac{\tilde\delta_0}{\tilde\delta_c}\frac{D(a)}{D(a_0)}\right]^{\tilde\delta_{\rm c}/3}\,. \end{aligned} \tag{C9}$$

where the curvature of the perturbation is parametrized by its extrapolated linear density contrast at the present epoch, $\tilde\delta_0$. Note that for overdensities which expand forever, $\tilde\delta_0>0$ and $a_{\rm p}<a$, while for underdensities $\tilde\delta_0<0$ and $a_{\rm p}>a$. Also, because $D(a)$ asymptotes to a constant value for $a\to\infty$ (as we will see in the next sections) , $a_{\rm p}$ grows proportionally to a at late times. This is the exponential expansion phase, described in our analysis above.

c. *Solutions of the Evolution Equation*

For eventually collapsing structures ($\kappa\geq\kappa_{\rm min,coll}$), separation of variables in equation C5 and integration yields,

$$\int_0^a\frac{\sqrt{y}dy}{\sqrt{\omega y^3+1}}=\begin{cases}\int_0^{a_{\rm p}}\frac{\sqrt{x}dx}{\sqrt{\omega x^3-\kappa x+1}} & a<a_{\rm ta}\\ 2\int_0^{a_{\rm p,ta}}\frac{\sqrt{x}dx}{\sqrt{\omega x^3-\kappa x+1}}-\int_0^{a_{\rm p}}\frac{\sqrt{x}dx}{\sqrt{\omega x^3-\kappa x+1}} & a\geq a_{\rm ta}\end{cases}, \tag{C10}$$

where $a_{\rm ta}$ is the cosmic epoch when $a_{\rm p}=a_{\rm p,ta}$. Now the integral on the LHS of equation C10 can be calculated using [9]

$$\int\frac{\sqrt{y}dy}{\sqrt{\omega y^3+1}}=\frac{2}{3}\omega^{-1/2}\sinh^{-1}\sqrt{\omega y^3}\,. \tag{C11}$$

The integral of the RHS can be re-written as

$$\int_0^{a_{\rm p}}\frac{\sqrt{x}dx}{\sqrt{\omega x^3-\kappa x+1}}=\frac{2}{3}\omega^{-1/2}\mathcal{V}_1(r,\mu) \tag{C12}$$

where $\mathcal{V}_1$ is the *incomplete vacuum integral of the first kind*, defined in appendix D, and

$$r=a_{\rm p}/a_{\rm p,ta}\,,\qquad \mu=(\omega a_{\rm p,ta}^3)^{-1}\,. \tag{C13}$$

Note that for this range of curvature values, $\kappa/\omega^{1/3}$ (which is the quantity which parametrizes the behavior of the perturbation with time) is a function of μ alone, with

$$\kappa/\omega^{1/3} = (1+\mu)/\mu^{2/3}\,. \tag{C14}$$

Using equations C11 and C12, equation C10 can be rewritten as,

$$a = \begin{cases} \omega^{-1/3}\left\{\sinh\left[\mathcal{V}_1(r,\mu)\right]\right\}^{2/3}\,, & a \le a_{\rm ta} \\ \omega^{-1/3}\left\{\sinh\left[2\mathcal{V}_1(1,\mu) - \mathcal{V}_1(r,\mu)\right]\right\}^{2/3}\,, & a > a_{\rm ta} \end{cases}\,. \tag{C15}$$

Equation C15 is the spherical evolution solution for a collapsing perturbation with amplitude κ (parametrized above by μ) in an $\Omega_\Lambda + \Omega_{\rm m} = 1$, $\Omega_\Lambda/\Omega_{\rm m} = \omega$ universe, and gives r (and hence $a_{\rm p}$) as a function of a for this model. Note that $\mathcal{V}_1(r,\mu)$ is the development angle for this cosmology.

The scale factor of the universe at turnaround for a given collapsing overdensity can be found immediately from equation C15,

$$a_{\rm ta} = \omega^{-1/3}\left[\sinh\mathcal{V}_1(1,\mu)\right]^{2/3}\,. \tag{C16}$$

The scale factor of the universe at collapse, $a_{\rm coll}$ (when the scale factor of the perturbation becomes formally zero, $a_{\rm p,c} = r_{\rm c} = 0$) is, from equation C15 and since $\mathcal{V}_1(0,\mu) = 0$,

$$a_{\rm coll} = \omega^{-1/3}\left[\sinh 2\mathcal{V}_1(1,\mu)\right]^{2/3}\,. \tag{C17}$$

Equation C15 should not be applied "literally" until the final collapse of the perturbation to a singularity, since the physical picture for the late stages of the evolution of a perturbation involves virialization at a finite radius. It has been shown by [30] that the analogous arguments which give $a_{p,v} = a_{p,ta}/2$ for the $\Omega_{\rm m} = 1$ cosmology give, for an $\Omega_{\rm m} + \Omega_\Lambda = 1$ universe,

$$4\omega a_{\rm p,v}^3 - \frac{2+2\omega a_{p,ta}^3}{a_{p,ta}} a_{p,v} + 1 = 0\,. \tag{C18}$$

The physically meaningful solution of C18 which gives the correct behavior for $\omega \to 0$ is (using eq. C13)

$$a_{\rm p,v} \;=\; a_{\rm p,ta}\sqrt{\frac{2\mu+2}{3}}\cos\frac{1}{3}\left(\cos^{-1}\sqrt{\frac{27\mu^2}{(2\mu+2)^3}} + \pi\right)\,. \tag{C19}$$

The scale factor $a_{\rm v}$ of the universe when the scale factor of the perturbation *past its turnaround* becomes equal to $a_{\rm p,v}$, will be given by the second branch of equation C15, for $a_{\rm p} = a_{\rm p,v}$. Then, the validity range for the second branch of equation C15 is $a_{\rm ta} < a < a_{\rm v}$.

For $a > a_{\rm v}$, we can no longer use the spherical evolution solution to describe the physical picture of interest (virialization). In the next section we will present a simple recipe we will use to follow the late stages of evolution of the perturbation which satisfies the desired boundary conditions ($a_{\rm p} = a_{\rm p,v}$ at $a_{\rm coll}$ and constant thereafter).

For perpetually expanding structures ($\kappa < \kappa_{\rm min,coll}$), equation C5 gives

$$\int_0^a \frac{\sqrt{y}dy}{\sqrt{\omega y^3+1}} = \int_0^{a_{\rm p}} \frac{\sqrt{x}dx}{\sqrt{\omega x^3 - \kappa x + 1}}\,. \tag{C20}$$

In this case, the integral on the RHS can be rewritten as

$$\int_0^{a_{\rm p}} \frac{\sqrt{x}dx}{\sqrt{\omega x^3 - \kappa x + 1}} = \frac{2}{3}\omega^{-1/2}\mathcal{H}_1(r,\varpi) \tag{C21}$$

where $\mathcal{H}_1$ is the *hyperbolic vacuum integral of the first kind*, defined in appendix D, and

$$r = a_{\rm p}/|a_{\rm p,R}|\,, \qquad \varpi = (\omega|a_{\rm p,R}|^3)^{-1}\;, \tag{C22}$$

where $a_{\rm p,R}$ is the only real (and always negative) root of equation C3 when $\kappa < \kappa_{\rm min,coll}$,

$$a_{\rm p,R} = \frac{-\omega^{\frac{1}{3}}}{\sqrt[3]{\left(\frac{1}{2} - \sqrt{\frac{1}{4} - \frac{\kappa^3}{27\omega}}\right)^2} + \sqrt[3]{\left(\frac{1}{2} + \sqrt{\frac{1}{4} - \frac{\kappa^3}{27\omega}}\right)^2} - \frac{\kappa}{3\omega^{\frac{1}{3}}}} \tag{C23}$$

As in the case of collapsing perturbations, $\kappa/\omega^{1/3}$ is a function of ϖ alone, with

$$\kappa/\omega^{1/3} = (1-\varpi)/\varpi^{2/3}\,. \tag{C24}$$

Then, $\varpi = 1$ is a flat subuniverse (not perturbed with respect to the background), and perturbations with $\varpi > 1$ are underdensities while $1/4 < \varpi < 1$ correspond to non-collapsing overdensities.

Then, equation C20 becomes

$$a = \omega^{-1/3}\left\{\sinh\left[\mathcal{H}_1(r,\varpi)\right]\right\}^{2/3} \tag{C25}$$

which is the spherical evolution solution for a non-collapsing perturbation with amplitude κ (parametrized above by ϖ) in an $\Omega_\Lambda + \Omega_{\rm m} = 1$, $\Omega_\Lambda/\Omega_{\rm m} = \omega$ universe. As for collapsing perturbations, $\mathcal{H}_1(r,\varpi)$ is the development angle.

2. $\tilde{\delta}_0(\delta)$ according to the spherical evolution model

The linear theory result for a growing-mode perturbation in an $\Omega_{\rm m} + \Omega_\Lambda = 1$ cosmology is [31]

$$\tilde{\delta} = \tilde{\delta}_0 \frac{D(a)}{D(a_0)} \tag{C26}$$

where D, the linear growth factor, is given by $D(a) = A[(2\omega)^{1/3}a]$ with

$$A(x) = \frac{(x^3+2)^{1/2}}{x^{3/2}}\int_0^x \left(\frac{u}{u^3+2}\right)^{3/2} du\,. \tag{C27}$$

To find the relation between $\tilde{\delta}_0$ and κ, we expand the exact ($\delta = a^3/a_{\rm p}^3 - 1$) and linear relations for the overdensity to first order in a and demand that the coefficients be equal. Thus we get [9]

$$\kappa = \frac{(2\omega)^{1/3}}{3A\left[(2\omega)^{1/3}a_0\right]}\tilde{\delta}_0 = \frac{(2\omega)^{1/3}}{3A\left[(2\omega)^{1/3}\right]}\tilde{\delta}_0\,, \qquad \text{(C28)}$$

since $a_0 = 1$. This is the value of the constant κ for a perturbation which at a cosmic epoch $a_0 = 1$ has a linearly extrapolated overdensity $\tilde{\delta}_0$. Note that since the linear theory result is the same for both underdensities and overdensities, equation C28 holds for both cases. For underdensities, both κ and $\tilde{\delta}$ will be negative, while for overdensities both will be positive.

At any given epoch a, there is a unique perturbation (parametrized by κ or, equivalently, by μ or ϖ) which will have achieved a true density contrast δ at that time. Therefore, to calculate the desired conversion relation $\tilde{\delta}_0(a,\delta)$ we first calculate κ (or, equivalently, μ or ϖ) from the given a and δ and the appropriate solution of the evolution equation (C15 or C25). Then, we use equation C28 to evaluate $\tilde{\delta}_0$.

To determine which is the appropriate solution of the evolution equation we need to use for each δ, we calculate the limits of applicability of each equation in terms of δ.

- Equation C25 is applicable for all forever expanding perturbations. For any given epoch a, the maximum density contrast of such perturbations is achieved by the Eddington perturbation and is equal to $\delta_{\rm Ed}(a)$, given in line 1 of Table II. Then, the applicability domain of equation C25 is $-1 < \delta \leq \delta_{\rm Ed}(a)$, and the conversion relation in this case takes the form shown in the 1st line of Table III.

- The first branch of equation C15 is applicable for eventually collapsing perturbations which, however, have not reached their turnaround radius yet. The maximum δ of all such perturbations at a given a is achieved by the perturbation which is turning around at a, and is equal to $\delta_{\rm ta}(a)$, given in line 2 of Table II. The applicability domain of the first branch of equation C15 is then $\delta_{\rm Ed}(a) < \delta \leq \delta_{\rm ta}(a)$ and the conversion relation in this case is shown in the 2nd line of table III.

- The second branch of equation C15 is applicable for eventually collapsing perturbations which are past their turnaround but which have not yet reached their virial radius. The maximum δ of such perturbations at a given a is achieved by the perturbation which is reaching its virial size at a, and is equal to $\delta_{\rm v}(a)$, given in line 3 of Table II. The applicability domain of the second branch of equation C15 is then $\delta_{\rm ta}(a) < \delta \leq \delta_{\rm v}(a)$ and the conversion relation in this case is shown in the 3rd line of table III.

- Perturbations which have reached their virial size but have not yet reached their designated collapse time, $a_{\rm coll}(\mu)$, need to be treated separately, since the spherical collapse model fails (does not agree with the physical picture we would like to describe, although it is still formally applicable) for radii smaller than the virial radius. Since a realistic description of the microphysical dissipation processes which lead to virialization is far beyond the scope of this analytical calculation, we will adopt a prescription which is driven by mathematical simplicity. We will assume that for $\delta_{\rm v}(a) < \delta \leq \delta_{\rm c}(a)$ the conversion relation $\tilde{\delta}_0(a,\delta)$ has the simplest polynomial form which satisfies the following physically motivated boundary conditions:

  – The extrapolated overdensity is continuous and smooth at $\delta_{\rm v}$, so $\tilde{\delta}_0(a,\delta_{\rm v}) = \tilde{\delta}_{0,{\rm v}}$ and $\partial\tilde{\delta}_0/\partial\delta\Big|_{\delta_{\rm v}} = \tilde{\delta}'_{0,{\rm v}}$ as given by the appropriate relations of the previous branch (3rd line of tables III and IV correspondingly).

  – After time $a_{\rm coll}(\mu)$ the radius of the perturbation remains constant and equal to the virial radius so changes in the (true) overdensity are only due to the increase of the scale factor of the background universe. This then implies that $\tilde{\delta}_0(a,\delta_{\rm c}) = \tilde{\delta}_{0,{\rm c}}$ given by equation C29 and $\partial\tilde{\delta}_0/\partial\delta\Big|_{\delta_{\rm c}} = (\partial\tilde{\delta}_0/\partial\mu|_{\mu_{\rm c}})(\partial\mu/\partial\delta|_{\delta_{\rm c}}) = \tilde{\delta}'_{0,{\rm c}}$ given in Table III line 4.

  The conversion relation in this case is shown in Table III line 4,while its applicability domain is $\delta_{\rm v}(a) < \delta \leq \delta_{\rm c}(a)$, with $\delta_{\rm c}(a)$ given in Table II line 4. Past their collapse time, perturbations are treated as virialized objects without substructure and are not relevant as "local environment" of other objects for the purposes of our double distribution calculation, hence it is not necessary to have a conversion relation of $\delta > \delta_{\rm c}(a)$. The calculation would be simplified (this last branch would be unnecessary) if we chose to regard perturbations as virialized objects after the moment they reached their virial size after turnaround, at time a_v. However, we will retain the usual assumption that objects virilize at time $a_{\rm coll}$ for consistency with existing Press-Schechter calculations.

3. Critical extrapolated overdensity for collapse, $\tilde{\delta}_{0,{\rm c}}(a)$

We need to find the critical $\tilde{\delta}_{0,{\rm c}}(a)$ for collapse if the field is linearly extrapolated to the present epoch, i.e. the value the linearly extrapolated to the present overdensity must have, for a structure to have collapsed at universe scale factor a. This, from equation C28, will be

$$\tilde{\delta}_{0,{\rm c}}(a) = \frac{3A\left[(2\omega)^{1/3}\right]}{(2)^{1/3}}\frac{1+\mu_{\rm c}(a)}{\left[\mu_{\rm c}(a)\right]^{2/3}} \qquad \text{(C29)}$$

TABLE II: Applicability limits for different branches of the spherical evolution solution

Limit	Expression	Auxiliary Relations
Density contrast of Eddington overdensity, $\delta_{\rm Ed}(a)$	$\delta_{\rm Ed}(a) = 2\omega\left(\frac{a}{r_{\rm Ed}(a)}\right)^3 - 1$	$\sinh^{-1}\sqrt{\omega a^3} - \mathcal{V}_1(r_{\rm Ed}, 2) = 0$
Density contrast of overdensity turning around at a, $\delta_{\rm ta}(a)$	$\delta_{\rm ta}(a) = \omega a^3 \mu_{\rm ta}(a) - 1$	$\sinh^{-1}\sqrt{\omega a^3} - \mathcal{V}_1(1, \mu_{\rm ta}) = 0$
Density contrast of overdensity reaching its virial size at a, $\delta_{\rm v}(a)$	$\delta_{\rm v}(a) = \left(\frac{a}{a_{\rm p,v}[\mu_{\rm v}(a)]}\right)^3 - 1$	$\sinh^{-1}\sqrt{\omega a^3} - 2\mathcal{V}_1(1,\mu_{\rm v}) + \mathcal{V}_1\left[r_{\rm v}(\mu_{\rm v}), \mu_{\rm v}\right] = 0$ $r_{\rm v}(\mu) = a_{\rm p,v}(\mu)/a_{\rm p,ta}(\mu)$
Density contrast of virialized overdensity formally collapsing to a point at a, $\delta_{\rm c}(a)$	$\delta_{\rm c}(a) = \left[\frac{a}{a_{\rm p,v}[\mu_{\rm c}(a)]}\right]^3 - 1$	$\sinh^{-1}\sqrt{\omega a^3} - 2\mathcal{V}_1(1,\mu_{\rm c}) = 0$

TABLE III: Different branches of conversion relation $\tilde{\delta}_0(a,\delta)$ for an $\Omega_{\rm m} + \Omega_\Lambda = 1$ universe.

Branch	$\tilde{\delta}_0(\delta, a)$	Auxiliary relations
$-1 < \delta \le \delta_{\rm Ed}$	$\tilde{\delta}_0(a,\delta) = \frac{3A\left[(2\omega)^{1/3}\right]}{2^{1/3}} \frac{1-\varpi(a,\delta)}{[\varpi(a,\delta)]^{2/3}}$	$\sinh^{-1}\sqrt{\omega a^3} - \mathcal{H}_1\left[a\left(\frac{\varpi\omega}{1+\delta}\right)^{1/3}, \varpi\right] = 0$
$\delta_{\rm Ed} < \delta \le \delta_{\rm ta}$	$\tilde{\delta}_0(a,\delta) = \frac{3A\left[(2\omega)^{1/3}\right]}{2^{1/3}} \frac{1+\mu(a,\delta)}{[\mu(a,\delta)]^{2/3}}$	$\sinh^{-1}\sqrt{\omega a^3} - \mathcal{V}_1\left[a\left(\frac{\mu\omega}{1+\delta}\right)^{1/3}, \mu\right] = 0$
$\delta_{\rm ta} < \delta \le \delta_{\rm v}$	$\tilde{\delta}_0(a,\delta) = \frac{3A\left[(2\omega)^{1/3}\right]}{2^{1/3}} \frac{1+\mu(a,\delta)}{[\mu(a,\delta)]^{2/3}}$	$\sinh^{-1}\sqrt{\omega a^3} - 2\mathcal{V}_1(1,\mu) + \mathcal{V}_1\left[a\left(\frac{\mu\omega}{1+\delta}\right)^{1/3}, \mu\right] = 0$
$\delta_{\rm v} < \delta \le \delta_{\rm c}$	$\tilde{\delta}_0(a,\delta) = \tilde{\delta}_{0,\rm v} + \tilde{\delta}'_{0,\rm v}(\delta-\delta_{\rm v}) + \frac{3(\tilde{\delta}_{0,\rm c}-\tilde{\delta}_{0,\rm v})-(\delta_{\rm c}-\delta_{\rm v})(2\tilde{\delta}'_{0,\rm v}+\tilde{\delta}'_{0,\rm c})}{(\delta_{\rm c}-\delta_{\rm v})^2}(\delta-\delta_{\rm v})^2 + \frac{(\tilde{\delta}'_{0,\rm c}+\tilde{\delta}'_{0,\rm v})(\delta_{\rm c}-\delta_{\rm v})-2(\tilde{\delta}_{0,\rm c}-\tilde{\delta}_{0,\rm v})}{(\delta_{\rm c}-\delta_{\rm v})^3}(\delta-\delta_{\rm v})^3$	$\tilde{\delta}_{0,\rm v} = \tilde{\delta}_0(a,\delta_{\rm v})$, given in this Table line 3 $\tilde{\delta}'_{0,\rm v} = \frac{\partial\tilde{\delta}_0}{\partial\delta}\Big\vert_{\delta_{\rm v}}$, given in Table IV line 3 $\tilde{\delta}_{0,\rm c} = \tilde{\delta}_0(a,\delta_{\rm c})$, given by equation C29 $\tilde{\delta}'_{0,\rm c} = \frac{\partial\tilde{\delta}_0}{\partial\delta}\Big\vert_{\delta_{\rm c}} = -\frac{A\left[(2\omega)^{1/3}\right]\left(6\omega^{2/3}a_{\rm p,v}^2\mu_{\rm c}^{2/3}-1-\mu_{\rm c}\right)}{\left(2\mu_{\rm c}^2\right)^{1/3}(\delta_{\rm c}+1)}$ $\mu_{\rm c}(a)$ given in Table II line 4.

where again $\mu_{\rm c}(a)$ is given by Table II line4.

The dependence of $\tilde{\delta}_{0,\rm c}$ on a can also be expressed in terms of the linear growth factor, $D(a)$, as was the case for the $\Omega_{\rm m} = 1$ universe. The conversion relation between $\delta(a)$ and $\tilde{\delta}_a$ (the linear-theory result for the density contrast at time a) is independent of a. In other words, as long as δ and $\tilde{\delta}$ both refer to the same time, knowledge of the one uniquely defines the other, independently of the actual time at which they are both evaluated. As $\delta(a) \to \infty$, $\tilde{\delta}_a \to \tilde{\delta}_{\rm c}$, the linear-theory density contrast at the time of collapse (given by eq. C29 for $a = 1$). Therefore $\tilde{\delta}_{\rm c}$ is the same for perturbations of all curvatures, and, using equation C26, we can write

$$\tilde{\delta}_{0,\rm c}(a_{\rm coll}) = \tilde{\delta}_{\rm c}\frac{D(a_0)}{D(a_{\rm coll})}\,. \tag{C30}$$

4. $\partial\tilde{\delta}_0/\partial\delta|_a$

In addition to the relation between δ and $\tilde{\delta}_0$, we will also need the derivative $\partial\tilde{\delta}_0/\partial\delta|_a$ in order to convert between true and extrapolated overdensity differentials in equation (16). The calculation is similar as in the case of an $\Omega_{\rm m} = 1$ universe, and the results are summarized in table IV.

In table IV, $\mathcal{H}_2(r,\varpi)$ is the *hyperbolic vacuum integral of the second kind*, and $\mathcal{V}_2(r,\mu)$ is the *incomplete vacuum integral of the second kind*, defined in appendix D.

APPENDIX D: VACUUM INTEGRALS

Due to the central importance and frequent use of vacuum integrals in this calculation, we have generated numerical functions based on combinations of tabulated values and asymptotic approximations which evaluate each of the vacuum integrals in a small fraction of the time that would be required for quadrature, and with an accuracy better than 0.5% throughout their domains. These functions are publicly available at `http://www.astro.uiuc.edu/~bdfields/DD`.

1. The incomplete vacuum integral of the first kind $\mathcal{V}_1$

a. *Definition*

We define the incomplete vacuum integral of the first kind as

$$\mathcal{V}_1(r,\mu) = \frac{3}{2}\int_0^r \frac{\sqrt{x}dx}{\sqrt{(1-x)(-x^2-x+\mu)}}\,, \tag{D1}$$

with domain $0 \le r \le 1$ and $\mu \ge 2$.

TABLE IV: Different branches of derivative $\partial\tilde{\delta}_0/\partial\delta|_a$ for an $\Omega_{\rm m}+\Omega_\Lambda=1$ universe.

Branch	**Auxiliary Function**	$\boldsymbol{\partial\tilde{\delta}_0/\partial\delta\Big\vert_a\ (a,\delta)=}$	**Definitions of Additional Functions**
$-1<\delta\le\delta_{\rm Ed}$	$\Phi_1=\sinh^{-1}\sqrt{\omega a^3}-\mathcal{H}_1(r,\varpi)$	$-\frac{\partial\Phi_1}{\partial\delta}\left(\frac{\partial\Phi_1}{\partial\tilde{\delta}_0}\right)^{-1}$	$\frac{\partial\Phi_1}{\partial\delta}=\frac{a^{3/2}}{2(1+\delta)^{3/2}\sqrt{\frac{a^3}{(1+\delta)}-\frac{a(\varpi-1)}{\varpi^{2/3}(1+\delta)^{1/3}}+\frac{1}{\omega}}}$ $\frac{\partial\Phi_1}{\partial\tilde{\delta}_0}=-\frac{(2\varpi^2)^{1/3}}{3A[(2\omega)^{1/3}]}\mathcal{H}_2\left[a\left(\frac{\varpi\omega}{1+\delta}\right)^{1/3},\varpi\right]$ $\sinh^{-1}\sqrt{\omega a^3}-\mathcal{H}_1\left[a\left(\frac{\varpi\omega}{1+\delta}\right)^{1/3},\varpi\right]=0$
$\delta_{\rm Ed}<\delta\le\delta_{\rm ta}$	$\Phi_2=\sinh^{-1}\sqrt{\omega a^3}-\mathcal{V}_1(r,\mu)$	$-\frac{\partial\Phi_2}{\partial\delta}\left(\frac{\partial\Phi_2}{\partial\tilde{\delta}_0}\right)^{-1}$	$\frac{\partial\Phi_2}{\partial\delta}=\frac{a^{3/2}}{2(1+\delta)^{3/2}\sqrt{\frac{a^3}{(1+\delta)}-\frac{a(\mu+1)}{\mu^{2/3}(1+\delta)^{1/3}}+\frac{1}{\omega}}}$ $\frac{\partial\Phi_2}{\partial\tilde{\delta}_0}=-\frac{(2\mu^2)^{1/3}}{3A[(2\omega)^{1/3}]}\mathcal{V}_2\left[a\left(\frac{\mu\omega}{1+\delta}\right)^{1/3},\mu\right]$ $\sinh^{-1}\sqrt{\omega a^3}-\mathcal{V}_1\left[a\left(\frac{\mu\omega}{1+\delta}\right)^{1/3},\mu\right]=0$
$\delta_{\rm ta}<\delta\le\delta_{\rm v}$	$\Phi_3=\ \sinh^{-1}\sqrt{\omega a^3}$ $-2\mathcal{V}_1(1,\mu)+\mathcal{V}(r,\mu)$	$-\frac{\partial\Phi_3}{\partial\delta}\left(\frac{\partial\Phi_3}{\partial\tilde{\delta}_0}\right)^{-1}$	$\frac{\partial\Phi_3}{\partial\delta}=-\frac{a^{3/2}}{2(1+\delta)^{3/2}\sqrt{\frac{a^3}{(1+\delta)}-\frac{a(\mu+1)}{\mu^{2/3}(1+\delta)^{1/3}}+\frac{1}{\omega}}}$ $\frac{\partial\Phi_3}{\partial\tilde{\delta}_0}=\frac{(2\mu^2)^{1/3}}{3A[(2\omega)^{1/3}]}\left\{\mathcal{V}_2\left[a\left(\frac{\mu\omega}{1+\delta}\right)^{1/3},\mu\right]-\frac{6\mu}{\mu-2}\frac{d\mathcal{V}_1(1,\mu)}{d\mu}\right\}$ $\sinh^{-1}\sqrt{\omega a^3}-2\mathcal{V}_1(1,\mu)+\mathcal{V}_1\left[a\left(\frac{\mu\omega}{1+\delta}\right)^{1/3},\mu\right]=0$
$\delta_{\rm v}<\delta\le\delta_{\rm c}$	—	$\tilde{\delta}'_{0,\rm v}+2\frac{3(\delta_{0,\rm c}-\tilde{\delta}_{0,\rm v})-(\delta_{\rm c}-\delta_{\rm v})(2\tilde{\delta}'_{0,\rm v}+\tilde{\delta}'_{0,\rm c})}{(\delta_{\rm c}-\delta_{\rm v})^2}(\delta-\delta_{\rm v})$ $+3\frac{(\tilde{\delta}'_{0,\rm c}+\tilde{\delta}'_{0,\rm v})(\delta_{\rm c}-\delta_{\rm v})-2(\tilde{\delta}_{0,\rm c}-\tilde{\delta}_{0,\rm v})}{(\delta_{\rm c}-\delta_{\rm v})^3}(\delta-\delta_{\rm v})^2$	with $\tilde{\delta}_{0,\rm c}$, $\tilde{\delta}_{0,\rm v}$ $\tilde{\delta}'_{0,\rm c}$, $\tilde{\delta}'_{0,\rm v}$, as in Table III line 4

b. Properties

Physically, $\mathcal{V}_1(r,\mu)$ is proportional to the time required by a perturbation of normalized curvature parameter $\kappa/\omega^{1/3}=(\mu+1)/\mu^{2/3}$ to achieve a size $a_{\rm p}=ra_{\rm p,ta}(\kappa/\omega^{1/3})$ *before turnaround*. Its asymptotic behavior for $r\ll 1$ is

$$\mathcal{V}_1(r,\mu)\overset{r\ll 1}{\approx}\frac{1}{\sqrt{\mu}}r^{3/2} \tag{D2}$$

while for $\mu\gg 1$ it is

$$\mathcal{V}_1(r,\mu)\overset{\mu\gg 1}{\approx}\frac{1}{\sqrt{2\mu}}\left[\frac{\pi}{2}-\sqrt{r(1-r)}-\sin^{-1}\sqrt{1-r}\right] \tag{D3}$$

In the case of the Eddington perturbation ($\mu=2$), we can derive a closed-form expression for $\mathcal{V}_1$:

$$\begin{aligned}\mathcal{V}_1(r,2) &= \frac{3}{2}\int_0^r\frac{\sqrt{x}dx}{(1-x)\sqrt{x+2}}\\ &= \frac{\sqrt{3}}{2}\left[\ln\frac{1+\sqrt{r}}{1-\sqrt{r}}-2\sqrt{3}\sinh^{-1}\sqrt{\frac{r}{2}}\right.\\ &\quad\left.+\ln\frac{2\sqrt{3}+\sqrt{3r}+3\sqrt{2+r}}{2\sqrt{3}-\sqrt{3r}+3\sqrt{2+r}}\right].\end{aligned} \tag{D4}$$

When $r=1$, the value of $\mathcal{V}_1(1,\mu)$ is the *complete* vacuum integral of the first kind, which is a function of μ alone. Physically, the complete vacuum integral of the first kind is proportional to the time required for a perturbation of curvature parametrized by μ to reach turnaround. The derivative of $\mathcal{V}_1(1,\mu)$ appears in the calculation of the derivative $\partial\tilde{\delta}_o/\partial\delta$, in the 3rd line of Table IV, and it is

$$\frac{d}{d\mu}\mathcal{V}_1(1,\mu)=-\frac{3}{4}\int_0^1\frac{\sqrt{x}dx}{\sqrt{1-x}(-x^2-x+\mu)^{3/2}}\,. \tag{D5}$$

2. The hyperbolic vacuum integral of the first kind $\mathcal{H}_1$

a. Definition

We define the hyperbolic vacuum integral of the first kind as

$$\mathcal{H}_1(r,\varpi)=\frac{3}{2}\int_0^r\frac{\sqrt{x}dx}{\sqrt{(1+x)(x^2-x+\varpi)}}\,, \tag{D6}$$

with domain $0\le r<\infty$ and $\varpi>1/4$.

b. Properties

Physically, $\mathcal{H}_1(r,\varpi)=$ is proportional to the time required by a perturbation of normalized curvature parameter $\kappa/\omega^{1/3}=(1-\varpi)/\varpi^{2/3}$ to achieve a size $a_{\rm p}=ra_{\rm p,R}(\kappa/\omega^{1/3})$. Its asymptotic behavior for $r\ll 1$ is

$$\mathcal{H}_1(r,\varpi)\overset{r\ll 1}{\approx}\frac{1}{\sqrt{\varpi}}r^{3/2} \tag{D7}$$

while for $r \gg 1$ it is

$$\mathcal{H}_1(r,\varpi) \overset{r\gg 1}{\approx} C(\varpi) + \frac{3}{2}\ln\left(2\sqrt{r^2-r+\varpi}+2r-1\right) \tag{D8}$$

where $C(\varpi)$ is a function dependent only on ϖ. In the case of a flat ($\varpi = 1$) perturbation, $\mathcal{H}_1$ can be integrated immediately to give

$$\mathcal{H}_1(r,1) = \frac{3}{2}\int_0^r \frac{\sqrt{x}dx}{\sqrt{x^3+1}} = \sinh^{-1}\sqrt{x^3}\,. \tag{D9}$$

3. The incomplete vacuum integral of the second kind $\mathcal{V}_2$

a. Definition

We define the incomplete vacuum integral of the second kind as

$$\mathcal{V}_2(r,\mu) = \frac{3}{4}\int_0^r \frac{x^{3/2}dx}{(1-x)^{3/2}(-x^2-x+\mu)^{3/2}}\,, \tag{D10}$$

with domain same as for $\mathcal{V}_1(r,\mu)$.

b. Properties

The incomplete vacuum integral of the second kind is related to $\mathcal{V}_1(r,\mu)$ through

$$\frac{\partial}{\partial(\kappa/\omega^{1/3})}\mathcal{V}_1(r,\mu) = \mu^{2/3}\mathcal{V}_2(r,\mu)\,, \tag{D11}$$

with

$$\kappa/\omega^{1/3} = (1+\mu)/\mu^{2/3}\,. \tag{D12}$$

In the case of the Eddington perturbation ($\mu = 2$), we can derive closed-form expressions for $\mathcal{V}_2$:

$$\begin{aligned}\mathcal{V}_2(r,2) &= \frac{3}{4}\int_0^r \frac{x^{3/2}dx}{(1-x)^3(x+2)^{3/2}} \\ &= \frac{\sqrt{3}}{72}\left[\frac{\sqrt{3r}(2-3r+4r^2)}{\sqrt{2+r}(1-r)^2}\right. \\ &\quad \left. + \log\frac{1-r}{1+2r+\sqrt{3r(2+r)}}\right]. \end{aligned} \tag{D13}$$

4. The hyperbolic vacuum integral of the second kind $\mathcal{H}_2$

a. Definition

We define the hyperbolic vacuum integral of the second kind as

$$\mathcal{H}_2(r,\varpi) = \frac{3}{4}\int_0^r \frac{x^{3/2}dx}{(1+x)^{3/2}(x^2-x+\varpi)^{3/2}}\,, \tag{D14}$$

and its domain is that of $\mathcal{H}_1(r,\varpi)$.

b. Properties

The hyperbolic vacuum integral of the second kind is related to $\mathcal{H}_1(r,\varpi)$ through

$$\frac{\partial}{\partial(\kappa/\omega^{1/3})}\mathcal{H}_1(r,\varpi) = \varpi^{2/3}\mathcal{H}_2(r,\varpi)\,, \tag{D15}$$

with

$$\kappa/\omega^{1/3} = (1+\varpi)/\varpi^{2/3}\,. \tag{D16}$$

In the case of a flat ($\varpi = 1$) perturbation, $\mathcal{H}_2$ takes the form

$$\mathcal{H}_2 = \frac{3}{2^{4/3}}\int_0^{2^{1/3}r}\left(\frac{u}{u^3+2}\right)^{3/2}du\,, \tag{D17}$$

which is the integral entering the linear growth factor in the $\Omega_{\rm m}+\Omega_\Lambda = 1$ universe. Hence, the linear growth factor function $A(x)$ can be written as

$$A(x) = \frac{2^{4/3}(x^3+2)^{1/2}}{3x^{3/2}}\mathcal{H}_2(2^{-1/3}x,1)\,. \tag{D18}$$